Norwegian University of Life Sciences

Master's Thesis 2023 60 ECTS
Faculty of Chemistry, Biotechnology and Food Science

The Role of Lactate and HCAR1 in Mitochondrial Dynamics and Neuronal Survival after Neonatal Hypoxia-Ischemia

Astrid Fanny Nordhei
Master of Science, Biotechnology

Acknowledgements

The work presented in this master thesis was done at the Department of Molecular Medicine at University of Oslo (UiO) and the Department of Microbiology at Oslo University Hospital (OUS) from August 2022 to May 2023 as a part of a master degree of Biotechnology at the Norwegian University of Life Sciences (NMBU).

First, I would like to express my gratitude to my supervisor, Johanne Egge Rinholm. Thanks for your excellent mentorship and always being available for guidance, both in the lab and in the writing process. Your passion for research and discovery has really inspired me. I am very grateful for having the opportunity to be a part of this research group and to be introduced to the world of neurospheres and brain research. I would also like to thank my internal supervisor Harald Carlsen for your guidance and practical help.

I would also like to give a big thanks to Emilie Glesaaen for guiding me all along this project. I am grateful for your patience, answering my numerous questions and the time you spent teaching me the techniques. Your expertise has been very valuable for shaping my understanding of the project. I would also like to thank Siri Egenæs for your tips and tricks in the lab and your funny anecdotes. I am also grateful for Luís Gonçalves who became my master sibling in the end. Your Portuguese treats were highly appreciated.

Lastly, I would also like to thank the phD community here at the physiology department for all the laughs and the interesting lunch topics. You really made this an inclusive and vibrant place.

Abstract

Neonatal Hypoxia-Ischemia (HI) is one of the most common causes for death and disabilities in infants. It is responsible for 23% of infant mortality and it affects 0.7-1.2 million neonates annually. Today the only treatment currently available is hypothermia. However, this treatment does not prevent all brain injury and many patients surviving HI develop neurological disorders such as seizures, hearing and vision loss in later years. Hence, further research is needed to develop new and effective treatments to reduce post-ischemic injury and to improve brain tissue regeneration.

Recent research from mouse models on HI has shown that the administration of lactate has a positive effect on recovery. In a paper published by our group it was discovered that the lactate receptor hydroxycarboxylic acid receptor 1 (HCAR1) plays and important role for cell proliferation and brain tissue repair after HI.

This study has revealed that HCAR1 does not only play a role in cell proliferation after HI, but that it could also play a role in the survival of mature neurons. By immunostaining on brain sections from mice exposed to HI, we found that the density of neurons was significantly lower in mice that lacked the HCAR1 receptor. Since mitochondrial metabolism is closely linked to neuronal survival and apoptosis, we then used differentiated neurospheres to test the effect of lactate on mitochondrial density in neurons. However, our experiments did not show any effect of lactate on the density or number of neuronal mitochondria. Finally, we used western blotting to determine whether HCAR1 can influence the expression of mitochondrial proteins after HI. Our data suggested that mice lacking HCAR1 have a reduced expression of a mitochondrial protein involved in respiration, but more data points are needed to confirm this finding. Hence, it is also possible that HCAR1 could be involved in other metabolic processes such as regulating the cell's energy metabolism and protein expression. Further research of HCAR1 in mouse models and in human tissue is important as this receptor as it is a therapeutic target for treatments against HI and possibly stroke in elderly people.

Sammendrag

Neonatal hypoksi-iskemi (HI) er en av de vanligste årsakene til død og funksjonshemming hos spedbarn. Det er ansvarlig for 23% av spedbarnsdødeligheten og det påvirker 0,7-1,2 millioner nyfødte årlig. Hypotermi den eneste behandlingen som er tilgjengelig i dag. Denne behandlingen forhindrer imidlertid ikke all hjerneskade, og mange pasienter som overlever HI utvikler nevrologiske lidelser som anfall, hørsel og synstap i senere år. Det er derfor et nødvendig med ytterligere forskning for å utvikle nye og effektive behandlinger for å redusere post-iskemisk skade og for å forbedre regenerering av hjernevev.

Nyere forskning på musemodeller for HI har vist at administrering av laktat har en positiv effekt på restitusjonen. I en artikkel publisert av vår gruppe ble det oppdaget at en reseptor for laktat, hydroksykarboksylsyre-reseptor 1 (HCAR1), spiller en viktig rolle for celleproliferasjon og reparasjon av hjernevev etter HI.

Denne studien har avslørt at HCAR1 ikke bare spiller en rolle i celleproliferasjon etter HI, men at den også kan spille en rolle i overlevelsen av modne nevroner. Ved å bruke immunmerking på hjernesnitt fra mus som var utsatt for HI fant vi at tettheten av nevroner var betydelig lavere hos mus som manglet HCAR1-reseptoren. Siden mitokondriell metabolisme er nært knyttet til nevronenes overlevelse og apoptose, brukte vi deretter differensierte nevrosfærer for å teste effekten av laktat på mitokondriell tetthet i nevroner. Imidlertid viste eksperimentene våre ingen effekt av laktat på tettheten eller antallet av nevronale mitokondrier. Avslutningsvis brukte vi western blotting for å bestemme om HCAR1 kan påvirke uttrykket av mitokondrielle proteiner etter HI. Våre data tydet på at mus som mangler HCAR1 har redusert uttrykk for et mitokondrielt protein involvert i respirasjon, men dette bør testes med flere datapunkter før det kan bekreftes. Derfor er det også mulig at HCAR1 kan være involvert i andre metabolske prosesser som å regulere cellens energimetabolisme og proteinuttrykk. Videre forskning av HCAR1 i musemodeller og i humant nervevev er viktig ettersom denne reseptoren kan være et mulig terapeutisk mål for behandlinger mot HI hos spedbarn og muligens hjerneslag hos eldre mennesker.

Abbreviations

ACADM: Acyl-Coenzyme A dehydrogenase

ACADVL: Acyl-Coenzyme A dehydrogenase very long chain

ATP: Adenosine triphosphate

bFGF: Basic fibroblast growth factor

BrdU: Bromodeoxyuridine

BSA: Bovine serum albumin

cAMP: Cyclic adenosine monophosphate

CCA: Common carotid artery

CNS: Central nervous system

COX4: Cytochrome c oxidase subunit 4

DAPI: 4′,6-diamidino-2-phenylindole

DG: Dentate gyrus

DMEM: Dulbecco's Modified Eagle Medium

EGF: Epidermal growth factor

ESC: Embryonic stem cell

GCPR: G-protein coupled receptor

GLUT: Glucose transporter

GPR81: G-protein-coupled receptor 81

HCAR: Hydroxycarboxylic acid receptor

HCAR1: Hydroxycarboxylic acid receptor 1

HCAR2: Hydroxycarboxylic acid receptor 2

HCAR3: Hydroxycarboxylic acid receptor 3

HI: Hypoxia-ischemia

ICC: Immunocytochemistry

IHC: Immunohistochemistry

KO: Knock out

LDH: Lactate dehydrogenase

MAP2: Microtubule associated protein 2

MCT: Monocarboxylate transporter

NADH: Nicotinamide adenine dinucleotide

NADPH: Nicotinamide adenine dinucleotide phosphate

NeuN: Neuronal nuclear protein

NF200: Neurofilament 200

NSA: Neurosphere assay

NSC: Neuronal stem cell

PBS: Phosphate-buffered saline

PBS-T: Phosphate-buffered saline-Tween

PCR: Polymerase chain reaction

PDL: Poly-D-Lysine

PFA: Paraformaldehyde

PFA: Paraformaldehyde

PVDF: Polyvinylidene fluoride

RT: Room temperature

SD: Standard deviation

SVZ: Sub-ventricular zone

TCA: Tricarboxylic Acid Cycle

TUJ1: Neuron-Specific class III beta-tubulin

WT: Wild type

Table of contents

1. Introduction

1.1 THE BRAIN AND THE CENTRAL NERVOUS SYSTEM

The central nervous system (CNS) includes the brain and the spinal cord. The brain can be divided into 3 main structures: the brainstem, the cerebrum, and the cerebellum. The cerebrum is the largest part (the large brain). The outermost part of the cerebrum is the neocortex, which is a folded surface made up of grey matter. The grey color comes from nerve cell bodies, or somas, which contain the nucleus and most of the cytoplasm. The cortex surrounds the white areas of the brain, also called white matter, which gets its color from the myelin of the myelinated axons [1].

Neurons and glial cells are important cells in the CNS. Neurons are responsible for sending electric signals while glial cells have a supportive role and are important for neuronal function. Glial cells are the most abundant cell group and include astrocytes, oligodendrocytes and microglia[2]. They are needed to maintain homeostasis, regulate synaptic activity and provide energy to the neurons.

1.2 NEURONAL DEVELOPMENT AND SIGNALING

Neurons develop from neural stem cells in a process called neurogenesis. Neurogenesis is the division of neural stem cells and their maturation into neural progenitor cells. These progenitor cells then migrate long distances and mature into neurons[3]. The early neuronal brain cells are called neuroepithelial cells and they develop into more elongated radial glial cells. From the radial glial cells, neurons can be generated directly or they can develop from the intermediate step called intermediate neural precursors [4]. Neurogenesis was previously thought to only be restricted to embryonic development, but it has also been detected in adulthood of various mammals in specific areas of the brain such as the hippocampus, an important structure for memory storage and formation[3].

Neurons have a complex structure made up of a soma, an axon, and dendrites. Most neurons have dendrites branching out from the soma and form a surface with a tree-like structure

(Figure 1). Neuronal signals can be transmitted from one cell to other surrounding or distant cells through contact points called synapses. A synapse is formed by an axon terminal of a pre-synaptic cell and part of a dendrite on a post-synaptic cell[5]. When neurotransmitter molecules are released from the axon terminal, the neurotransmitter can bind to receptors on the post-synaptic neuron. This can lead to the firing of an electric impulse (action potential) in the post-synaptic neuron. One neuron can form synapses with multiple neurons simultaneously. Oligodendrocytes provide myelin for the neurons, an insulating layer of fatty acids and proteins, which wraps around the axon and is crucial for faster conduction of the electrical impulses [1] The myelin sheath has gaps called Node of Ranvier in which the electrical impulse travel from one node to the next (Figure 1).

.

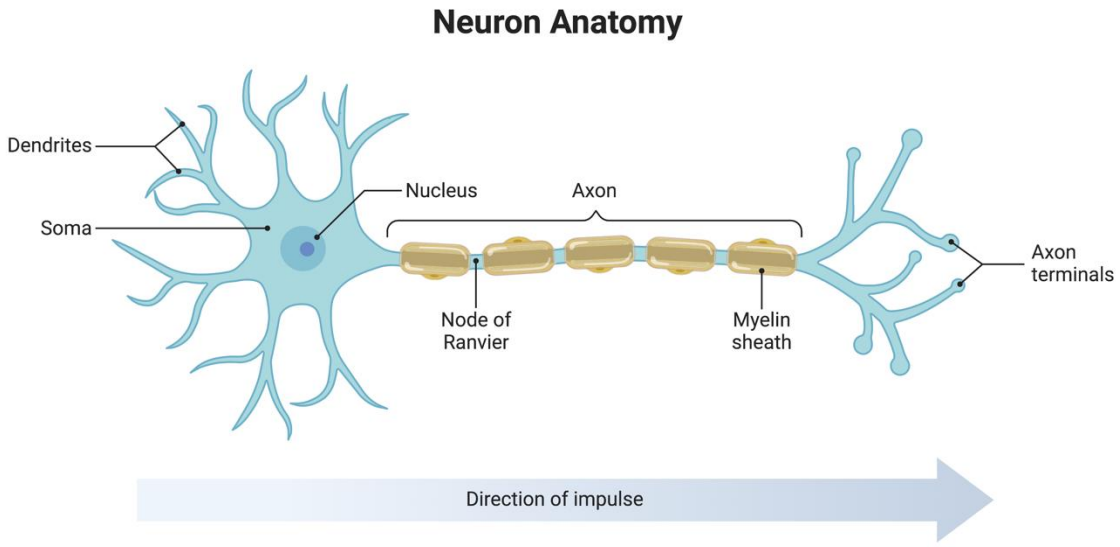

Figure 1: The structure of a neuron showing the nucleus and the dendrites extending out from the soma. The axon is covered by a myelin sheath allowing faster conduction of electrical impulses. The direction of the impulse is towards the axon terminals and the electrical impules is travelling in the Nodes of Ranvier, from one node to the next. This is called saltatory conduction. Made in BioRender.

1.3 ENERGY METABOLISM IN THE BRAIN

Although the brain only makes up 2% of the total body mass, it consumes around 20% of the total energy generated[6], [7]. Neurons are the cells with the highest energy demand as they use 80 to 90% of the total energy consumed by the brain[5]. Cellular energy in the form of adenosine triphosphate (ATP) is required to generate action potentials as well as postsynaptic potentials and for the maintenance of ion gradients and resting potentials. Most of the energy generated is used by the Na^+-K^+-ATPases, which pump sodium and potassium ions across the membrane against their concentration gradient. In addition, ATP also provides precursors for the biosynthesis of neurotransmitters [9].

Glucose is the primary energy source and is metabolized in the cells to generate ATP. There are different metabolic pathways that generate ATP, but oxidative phosphorylation, an oxygen-consuming pathway occurring in mitochondria, is the most efficient as it can generate up to 36 ATP molecules per glucose molecule. This mechanism starts with glucose entering the cells through glucose transporters. It is then broken-down during glycolysis, to produce 2 pyruvates, ATP and NADH. These pyruvates are further metabolized in the mitochondria to produce acetyl CoA, which then goes through the Krebs cycle, which yields ATP as well as electron donors for oxidative phosphorylation, where more ATP is generated. An overview of glucose and pyruvate metabolism are shown in figure 2.

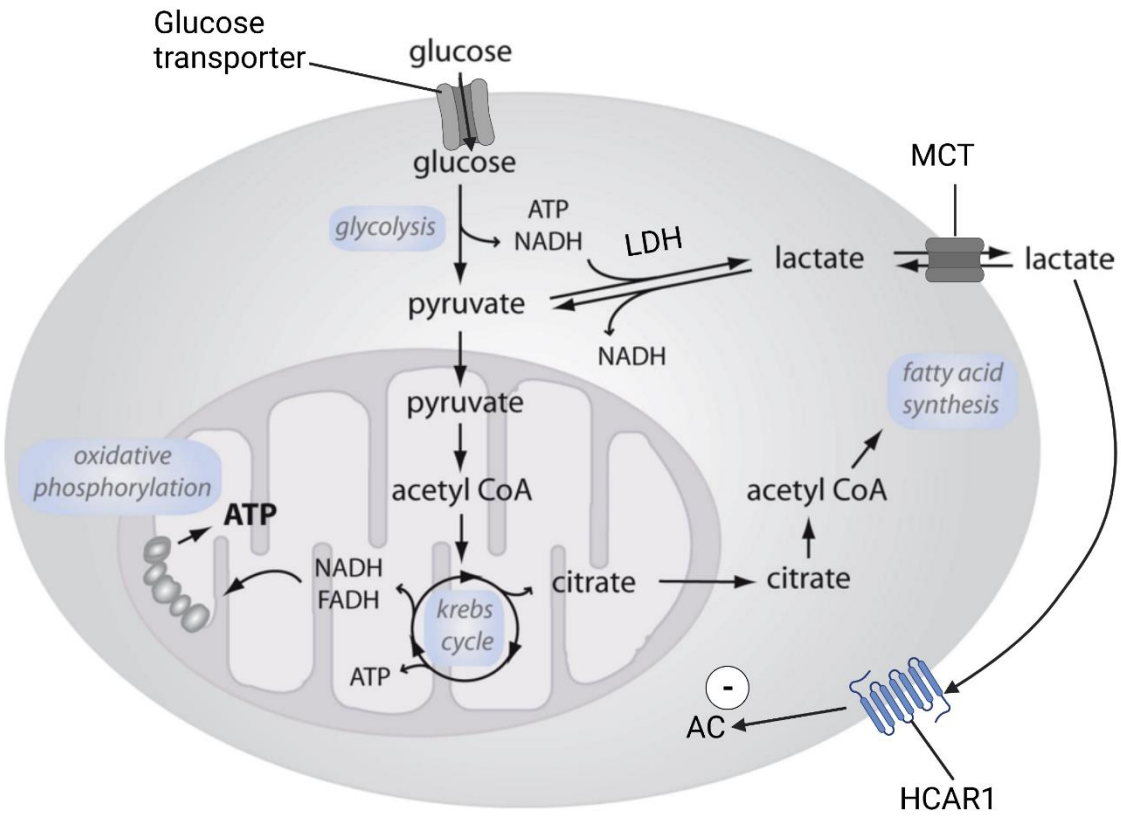

Figure 2: The metabolism of glucose, pyruvate and lactate in cells.

Glucose enters the cell through glucose transporters and is broken down through glycolysis to give 2 pyruvates and ATP. They can then enter the mitochondria and go through the Krebs cycle and oxidative phosphorylation to generate a large amount of ATP. Pyruvates can also be converted into lactate through the lactate dehydrogenase enzyme (LDH) and lactate can be released out of the cell and enter other cells through monocarboxylate transporters (MCTs). Lactate can alternatively activate the hydroxycarboxylic acid receptor 1 (HCAR1) which is negatively coupled to adenylyl cyclase (AC). Modified from Rinholm et al. (2014) [10].

1.4 MITOCHONDRIA AND MITOCHONDRIAL DYNAMICS

The mitochondrion is a large organelle composed of an outer membrane and a folded inner membrane. It has many important functions in cells such as generating ATP, buffering calcium ions in the cytosol and initiate certain types of apoptosis through the activation of a caspase signaling cascade (5). In neurons, most of the ATP is generated in the mitochondria through the TCA cycle and oxidative phosphorylation is used to reverse ion influxes after neurotransmission and action potentials[4].

Mitochondria are also dynamic structures, and their distribution correlates with the energy needs of the cell. In neurons, they are more densely distributed in regions with higher energy demands such as the pre- and post-synaptic domains of active synapses [7].

The mitochondria is a dynamic organelle and several recent studies have revealed the mechanisms controlling mitochondrial motility in neurons. It is now known that they move in every direction, pause, and stop [11]. Their anterograde transport (away from the soma) is mainly mediated by kinesins proteins KIF5 and KIF1B, while dynein motor proteins are responsible for their retrograde transport (towards the soma) [7]. The mobility of mitochondria has an activity-dependent regulation and is closely linked to the activity of neurons. Several factors can influence mitochondrial movement, including synaptic signaling (via intracellular calcium) and nutrient status[12]. Their mobility has been demonstrated to increase in dendrites where there are higher levels of ATP and to be inhibited where the level of ATP is lower. This suggests that the density of mitochondria in areas with higher ATP decrease as they will move to regions with decreased ATP concentrations [13], [14]In a study made by Pekkurnaz et al., they showed that glucose and the activation of O-GlcNAc Transferase (OGT), an enzyme whose activity depends on glucose availability, reduces anterograde and retrograde mitochondrial motility in neurons [15].

In addition to moving, mitochondria can also divide and fuse with each other[11]. By doing this the cell can regulate the number and the size of the mitochondria. This, in addition to the exchange of metabolites and mtDNA is important for the mitochondria to adapt to the varying energy demands of the cell [16]. Another important function of mitochondrial fission is to segregate old and damaged parts of the mitochondria, which can then be degraded through

mitophagy [17]. The fusion and fission events are mediated by GTPase proteins such as dynamin-related protein 1 (Drp1), mitofusin (Mfn) and optic dominant atrophy 1 (Opa1) [18]

Many studies have been done on mitochondrial dynamics because imbalances such as excessive fragmentations and blocked mitochondrial transport has been linked to many neurological diseases [18]. Furthermore, these imbalances can lead to impairments such as a decrease in energy production, reduced Ca^{2+} buffering or limitations in mitochondrial motility, which can all lead to neuronal cell death [16].

1.5 LACTATE AND LACTATE SHUTTLE

Lactic acid was first discovered in sour milk by Karl Wilhelm Scheele in 1780 and it was for a long time only considered a useless waste product formed through anaerobic glycolysis through physical exercise [8], [19]. In the 1950's McIlwain conducted an experiment which showed that lactate also functions as an energy substrate for neural cells, and it is now known also be an important signaling molecule to modulate neuronal functions[8].

Lactate is predominantly produced by astrocytes through glycolysis or glycogenolysis. During glycolysis, the pyruvate generated from the metabolism of glucose or glycogen, can also be converted into lactate by the enzyme lactate dehydrogenase (LDH)[8]. This lactate is then exported out of the cell through monocarboxylate transporters (MCTs) and can be imported into other cells and be converted back into pyruvate and go into the TCA cycle to generate ATP [10] (Figure 2).

The lactate shuttle was first described by Brooks in 1985 in a model which describes how lactate is transferred from lactate producing cells to lactate consuming cells [20]. This shuttling was observed between red and white fibers in muscle, but later a similar shuttle has been demonstrated between astrocytes and neurons in the brain and intracellularly between the cytosol and the mitochondria [8], [21].

Lactate is hence transferred to neurons when the energy demand is high to maintain neuronal function during high neuronal [8]. As neurons have a higher energy demand than other cells,

it is very likely that they will consume lactate in addition to glucose when available [10]. In a resting state, the levels of lactate in the brain are quite low. However, during physical exercise, lactate levels have been reported to increase up to 10-20 mM in the blood. This lactate can cross the blood brain barrier via MCTs and is consumed by the brain [8], [22].

1.6 HYDROXYCARBOXYLIC ACID RECEPTOR 1

The HCAR1 receptor, previously known as G-protein-coupled receptor 81 (GPR81), is a lactate receptor belonging to the G-protein coupled receptor family (GCPRs). The GCPRs is the largest receptor family with 800 genes coding for their proteins. Receptors from the GCPR family all share a common secondary structure consisting of seven transmembrane alpha helices separated by alternating intracellular and extracellular loops and a bound G protein. The binding of the G protein to a ligand leads to the activation of the receptor and the change of its conformation triggers different cell signaling cascades [23].

HCAR1 belongs to the subfamily called hydroxycarboxylic acid receptors (HCARs) which is composed of three members: HCAR1 (GPR81), HCAR2 (GPR109A) and HCAR3 (GPR109B). In humans, the GPCR family are located on chromosome 12. However, only HCAR1 and HCAR2 are expressed in rodents, and in mice they are located on chromosome 5. The HCAR family is unique because as they are made up of only one single exon and no introns. Furthermore, the HCAR1 receptor is the most evolutionary conserved receptor of the HCAR receptors as it has been found in all mammals and fish[24]. It was first found in adipose tissue to inhibit lipolysis by downregulating cAMP levels[25]. It has recently been discovered in the brain, but it is also found in several other tissues and cell types, including immune cells, and tumor cells[24]. In 2014, Lauritzen et al. demonstrated for the first time, the expression of functional HCAR1 receptors in the mouse brain. The authors suggested that the activation of HCAR1 through lactate is linked to energy metabolism, synaptic function, and blood flow in the brain [26] . In another paper, the same group also saw that the activation of HCAR1 receptor can lead to angiogenesis, which promotes neurogenesis and synaptic function [27]. Briquet et al found that HCAR1 downregulates the activity of neurons. By activating HCAR1 with an agonist, they found a decrease in neuronal spiking and excitatory post-synaptic currents in human cortical slices. Additionally, they also used patch clamping recording and found reduced excitability in the neurons of the hippocampus and cerebellum in

rats and mice. As HCAR1 downregulates synaptic activity. it also makes it a target for new treatment of epilepsy [28].

1.7 NEONATAL CEREBRAL HYPOXIA-ISCHEMIA

Brain injury due to hypoxia-ischemia (HI) is the leading cause of disability in newborn babies. It affects 0,7-1,2 million newborns and accounts for 23% of infant mortality per year[23]. HI occurs around or under birth when blood flow to the brain is temporarily blocked leading to an insufficient supply of oxygen and nutrients to the cells. To reduce damaged brain tissue after HI the infant's whole body or head can be cooled down to 33 C°. This is called hypothermic treatment but is not enough to prevent all brain injury. Infants who survive HI often get many different long-term effects and only 50-60% of HI survivors develop normally. Examples of these neurological symptoms are sensory or cognitive abnormalities and learning disorders. Hence, the development of new drugs is therefore necessary to help the recovery [14].

After HI, the neonatal brain can partly regenerate damaged brain tissue through stem cell proliferation, angiogenesis, and microglia-induced inflammation. Two recent studies found that mouse pups injected with lactate before or after HI had improved recovery [30], [31]. In a study published in 2022, our group showed that the absence of the HCAR1 receptor led to a decrease in the regeneration of brain tissue caused by reduced proliferation of neural stem progenitor cells and microglia activation. This makes HCAR1 a therapeutic target in the development of a treatment for neonatal HI [32].

1.8 METHODS USED TO STUDY THE BRAIN

Several different models are used in brain research. Studies of living human brains are mostly limited to non-invasive imaging techniques. Therefore, we need animal models or other in vitro systems to perform anatomical functional studies on a cellular level. Brains from animals can be used as models to better understand the human brain. Rodents such as mice or rats are often used due to their close resemblance to human brains and because they are relatively easy to breed. Other models include cell and tissue cultures such as embryonic stem cells, induced pluripotent stem cells, organotypic slice cultures and organoids to study brain development and disease. Neural stem cells can also be used in-vivo or in-vitro to develop therapeutic strategies and gain insights on the mechanisms surrounding neurological disorders.

In 1992, Reynolds and Weiss described a powerful in-vitro technique to study NSCs in a controlled environment called the neurosphere assay (NSA). In the adult brain, NSCs are mainly present in so called neurogenic niches in the sub-ventricular zone (SVZ) and the dentate gyrus (DG) regions of the brain. The isolation of NSCs comes usually from animals i.eg. mice or from human fetal brain and spinal cord [33]. The neurospheres are grown in a serum-free medium containing growth factors to stay undifferentiated and grow as floating spherical clusters called neurospheres. After the primary neurospheres have been in culture for a week they are passaged and can be further differentiated through removal of the growth factors [33].

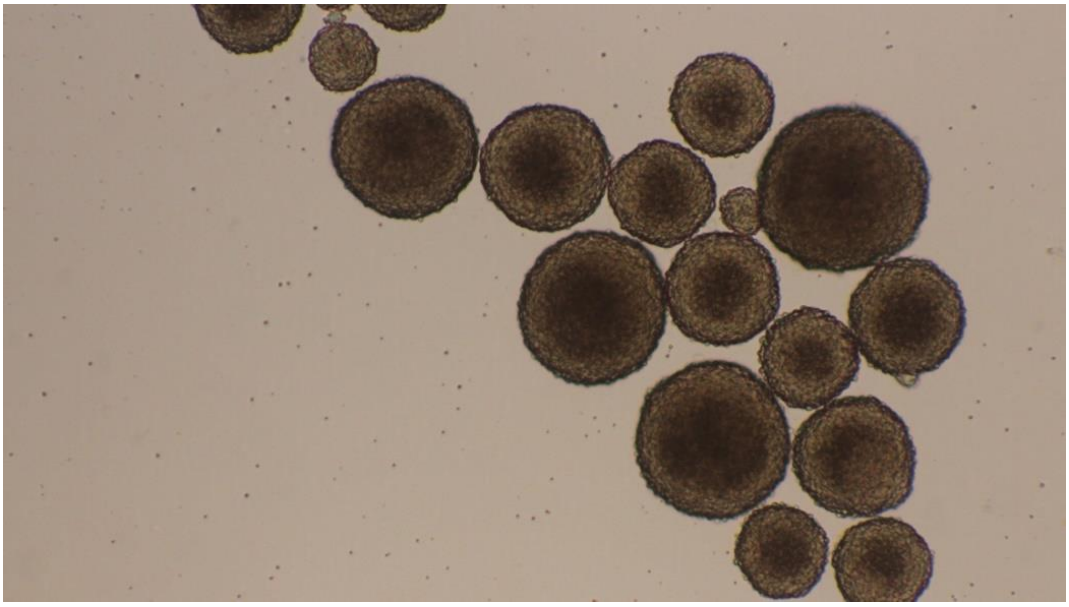

Figure 3: Image showing of a cluster of neurospheres

2. Aims and hypotheses

The previous work of our group and others has shown that lactate can improve recovery after hypoxia-ischemia (HI) via HCAR1, by stimulating proliferation of neural progenitors and other repair processes [32]. However, it is unknown whether stimulation of HCAR1 can influence the survival of neurons after HI. Moreover, since cell fate and –survival is closely associated with cell metabolism and mitochondria, a possible link between lactate and mitochondrial dynamics should be explored.

The overall aim of this thesis was to study a **possible role of lactate and HCAR1 in mitochondrial dynamics, mitochondrial protein expression and in neuronal survival after HI**.

Specifically, we aimed to answer the following questions:

1) Can the lactate receptor HCAR1 influence survival of neurons after hypoxia-ischemia?

Lactate was previously shown to be protective after ischemic events, but its effect on neuronal survival is unknown. **I hypothesize that neuronal survival after HI will be higher in mice that have HCAR1 compared with mice without the lactate receptor.**

2) Can a change in extracellular lactate concentration alter the density and/or size of mitochondria in neurons?

The size and the density of the mitochondria is closely linked to the cell's capacity to generate ATP. In line with this, elongated mitochondria have a higher rate of oxidative phosphorylation and ATP production than mitochondria with a small and rounded shape [34]. Lactate can be an important metabolite for neurons and may be able to influence the metabolic status of the cell. **I hypothesize that an increase in the extracellular lactate concentration will lead to more elongated mitochondria and an increase in the total neuronal area covered by mitochondria. I further hypothesize that this effect is mediated by the lactate receptor HCAR1.**

3) Does HCAR1 influence the expression of mitochondrial proteins?

If lactate and HCAR1 can influence mitochondrial size or density in a way that affects mitochondrial metabolism, then this should be reflected in the expression of mitochondrial proteins. In a previous study from our research group, the effect of HCAR1 was more pronounced after HI than under normal conditions[32]. I therefore also want to test the expression of mitochondrial proteins after HI. **I hypothesize that lower expression of mitochondrial proteins is found in the mice lacking HCAR1. I further hypothesize that the difference in mitochondrial protein expression between control mice and mice lacking HCAR1 will be larger after HI.**

3. Materials and methods

3.1 EXPERIMENTAL SETUP

.

1) **Investigate the survival of mature neurons after hypoxia-ischemia**

   Method: Immunohistochemistry with mature neural marker on coronal brain slices from mice from the previous work of our group. Confocal microscopy and quantification of mature neurons in the peri-infarct zone and the cortex.

2) **Testing the effect of extracellular lactate has on mitochondria density and size in neurons**

   Methods: Growing neurospheres from mouse brain and holding them in culture. Cell differentiation for 5 days then 24h incubation with 3mM lactate for treated cells and 3mM Na-Cl for control cells. Then immunostaining with neuronal and mitochondrial marker. Visualization with confocal microscopy.

3) **Investigate the levels of mitochondrial markers:**

   Methods: Protein extraction of the brain tissue followed by western blotting and staining of the membrane with mitochondria markers TOMM20, COX4, ACADM ACADVL.

3.2 ANIMALS

All the animals used in this study were HCAR1 knock-out (KO) and C57BL/6N wild-type (WT) mice. Neurospheres were made from heterozygous HCAR1 KO/WT mice (assumed to have a WT phenotype). The KO mice were obtained from Prof. Dr. Stefan Offermanns from the Max Planck institute for heart and lung research in Bad Nauheim, Germany and have been described previously [35].

Briefly, the HCAR1 KO line was made by homologous recombination in embryonic stem cells (ESCs). The gene coding for the HCAR1 receptor was removed by replacing the HCAR1 encoding exon with a cassette encoding for b galactosidase (LacZ) and neomycin resistance. The genotypes of the mice were verified with polymerase chain reaction (PCR). The animals were treated in accordance with the regional and ethical guidelines and the European Union's Directive 86/609/EEC.

3.3 INDUCING HYPOXIA-ISCHEMIA (HI)

9 days old mice underwent cerebral HI. This was performed by a technician in our lab and involved the permanent blocking of the left common artery followed by systemic hypoxia in an induction chamber.

Briefly explained, the mice were first anaesthetized with isoflurane and a skin incision was made in "the anterior midline of the neck" to expose the left common carotid artery (CCA). The artery was electrocoagulated with a monopolar cauterizer and then the neck incision was closed. After 1-2h, the mice were placed in a hypoxic atmosphere (10 % oxygen balance nitrogen: Yara) for 60 min at 36.0 degrees. The mice were then placed back in the cage with the dam until further experiments.

3.4 BrdU incorporation

The mice were injected with 0,1 mg/g of Bromodeoxyuridine (BrdU) into the peritoneum, 4-7 days after the HI at 24h intervals. Then, the brain was perfused and fixed for immunostaining.

3.5 Preparation of mouse tissue for immunostaining

7 days after induction of HI, the mice were anesthetized and transcardially perfused with 4% paraformaldehyde (PFA). Then, the brains were removed and stored in 4% PFA for 24h. This was followed by immersion fixation in 10% formalin before paraffin embedding. Lastly, 6-8 µm coronal brain sections were cut using a microtome. The preparation of the mouse tissue was performed by a fellow lab member. These sections were further stained using the immunohistochemistry method.

3.6 IMMUNOFLUORESCENCE

3.6.1 Immunocytochemistry and immunohistochemistry

Immunocytochemistry (ICC) and immunohistochemistry (IHC) are methods used to stain and visualize specific structures in a cell. These methods rely on specific antibody-antigen binding to localize and visualize target peptides or protein antigens in the cell. The difference between these methods is that IHC stains tissue samples, while ICC stains cells in a cell suspension or grown on a slide [36]. IHC was first used in 1942 when Coons and his colleagues used fluorescein-conjugated antibodies to localize pneumococcal antigens in infected tissues [37]. Now, it is an important tool in research as well as clinical diagnostics because it allows to study the expression of specific molecules in healthy and diseased cells [38]. Both IHC and ICC were used in this study.

IHC and ICC can stain tissue through the direct or the indirect method (illustrated in figure 2). In the direct method, a primary antibody has a marker, such as a fluorescent molecule directly attached to it. The antibody is applied to the tissue and binds to the protein of interest.

In the indirect method, the tissue is additionally treated with a secondary antibody targeted against the species in which the primary antibody was produced and is usually labeled with a marker. The secondary antibody binds to the primary antibody and the signal can be detected and visualized with a confocal microscope. Although being slightly more time consuming, the indirect method allows for higher signal amplification, the binding of many different antibodies, and lower antibody concentrations [27]. The indirect method was applied in this study and secondary antibodies that were connected to fluorophores were used. This specific technique is named immunofluorescence and allows for labeling several antigens simultaneously, using fluorophores that get excited at different wavelengths.

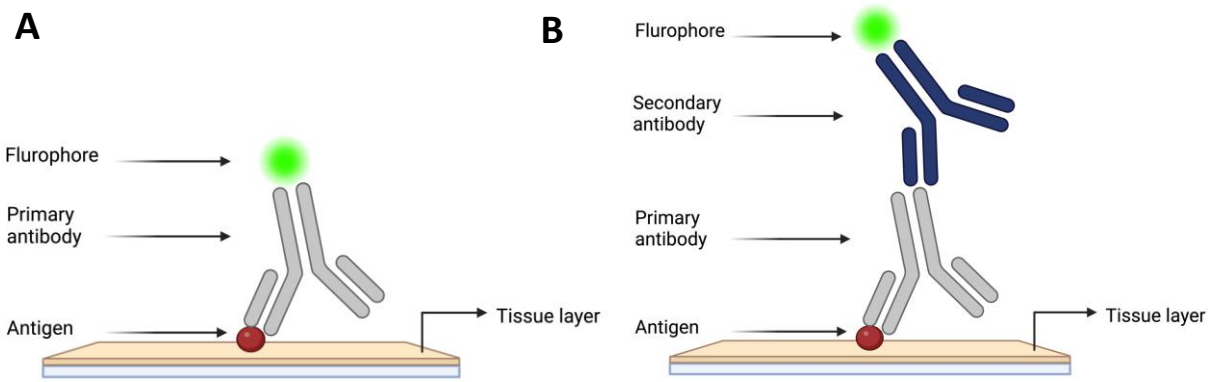

Figure 4: Illustration of the direct (A) and the indirect (B) method of immunohistochemistry.
A: A primary antibody with an attached fluorophore binds to a specific antigen in the tissue and gives off a detectable signal.
B: A primary antibody attaches to a specific antigen in the tissue. Then, a secondary antibody with an attached fluorophore binds to the primary antibody and gives signal amplification. Created in BioRender.com.

3.6.2 Protocol for IHC on cryostat sections

On the first day of this two-day protocol, the brain sections were taken out of the freezer and left to thaw at room temperature (RT). Antigen retrieval was performed for the sections which were stained with BrdU. Antigen retrieval started with the rinsing of sections with PBS for 10 minutes. Then, the sections were incubated for 20-30 minutes at 90 ºC with pre-heated citrate buffer (10 mM, pH 6.0). After this, the sections were left to cool down in room temperature for 10-20 minutes and then rinsed 2 x 10 minutes in PBS. The slides were carefully removed from the PBS and dried with kimwipes. Then, the sections were encircled with a PAP pen and left to dry a little. Blocking solution was added and the slides were incubated in a moisture chamber for 1h at RT. The sections were then incubated overnight with primary antibodies (Table B1 in the Appendix) in a moisture chamber at RT.

On the second day, the slides were rinsed 3 x 10 minutes in PBS and additional PAP pen was added around the brain sections if necessary. The sections were then incubated for 1h with the secondary antibodies and DAPI (Table B1 in the Appendix). The slides were again rinsed 3 x 10 minutes in PBS, dabbed dry and mounted with prolong gold. The slides were incubated at 4 ºC until observation in the confocal microscope.

3.7 The Neurosphere assay (NSA)

The NSA assay provides a source of renewable and undifferentiated CNS precursor cells, which can be easily expanded in culture. However, this cell culture is not homogenous and consists not only of NSCs but also of differentiated cells from the three neural lineages. During proliferation, these cells are cultured in a serum free medium with the growth factors epidermal growth factor (EGF) and basic fibroblast growth factor (bFGF). The NPCs are responsive to these mitogens, and when they are exposed to them, they enter a period of proliferation while the differentiated cells die [33], [39]. Upon removal of the growth factors the cells start to differentiate and can become neurons, oligodendrocytes, and astrocytes [40] .

3.7.1 Isolation and expansion of neurospheres

Primary neurospheres were made from the cerebrum of heterozygote C57BL/6N and KO mice on postnatal day 5. The mice were decapitated, and the cerebellum and olfactory bulb were removed. The dissected brain tissue was then triturated and cultured in 25T flasks containing proliferation medium of DMEM/F12 supplemented with 2mM glutamax, 20 ng/mL EGF and 10 ng/mL bFGF, B27 without vitamin A, N2 and penicillin/streptomycin. After 7 days in culture as free-floating aggregates, the neurospheres were split by disassociating them chemically with trypsin/EDTA and mechanically by trituration. They were added to a 75T flask and passaged every 7 days when they have reached a diameter of around 100 to 200 μm.

3.7.2 Neurosphere differentation

3.7.2.1 Optimalization

Some months prior and during this experiment a phD student from the lab worked with optimizing the method and to make the neurospheres differentiate on glass coverslips. This was challenging as the neurospheres seem to prefer plastic instead of glass and this led to them sticking more to the plastic around the coverslip. After several months this method seemed work and the plates were prepared the day before the experiment by putting the coverslips in each well and left open with the UV light on overnight.

3.7.2 Coating

The plate was coated with poly-D-lysine (PDL, 10 μg/mL) and incubated at 37 ºC for 2 hours.

3.7.3 Cell passage and differentiation

The protocol starts with the passage of the cells and ends with plating and differentiation. The cells were first transferred into a 50 mL falcon tube and spun at 170 x g for 5 minutes. The supernatant was then removed and 10 mL of DPBS was added to wash the cells. The cells were again spun at a 1000 rpm for 5 minutes. Then, the supernatant was removed and 1

mL of trypsin/EDTA was added. The cells were incubated for 10 minutes and taken out after 5 minutes to gently pipette up and down. After 10 minutes, 10 mL of 1% BSA/PBS was added to inactivate the trypsin and the cells were once again spun for 5 minutes. After this, the supernatant was removed, and 1 mL of differentiation medium was added. The cells were passed through a cell strainer and counted in duplicates.

The neurospheres were differentiated on passage number 3, when the neurospheres had reached a diameter of around 200 µm. For the differentiation, the cells were plated on a 24 well plate at a cell density of 5 x 10^4 cells/cm^2. 150 µL of cells + differentiation medium was added to each cover slip in each well and 350 µL of extra differentiation medium + FGF was added 3 hours later. The neurospheres were plated in differentiation medium for 5 days with daily half-medium changes. In addition, the cells were observed with a light microscope to check if they looked healthy and if they had differentiated.

3.8 Lactate incubation

On day 5 of differentiation, the plate of neurospheres was incubated for 24h with 3 mM Na-lactate diluted in differentiation medium or with 3 mM NaCl in differentiation medium for the control group.

3.9 Fixation

Fixation is an important step in tissue processing because it preserves the integrity and the structure of the cells. A fixative hardens cellular components and thereby prevents decomposition, autolysis, and putrefaction [41]. There are different types of fixatives, and they are arranged in 4 main groups: the aldehydes, the alcohols, the oxidizing, and the metallic fixatives [41], [42]. Aldehydes are the most used fixatives. They act by cross-linking proteins and cause the least loss of biochemical information. Organic fixatives have been found to cause loss of cell content and to damage the membrane by removing lipids [42].

After 24 hours of incubation in lactate or NaCl, the plated cells were fixed in 4% paraformaldehyde (PFA). This was done by removing the media from each well and adding

300 µL of 4% PFA (diluted in 1X PBS) to each well, and they were left to incubate for 10 minutes at RT. The wells were washed once with PBS and stored in 4 ºC until staining.

3.10 IMMUNOCYTOCHEMISTRY ON DIFFERENTIATED CELLS FROM NEUROSPHERES

After fixation, the cells were washed once with 300 µL 1X PBS, and further permeabilized by adding 300 µL of 0,1 % Triton-X/PBS and left to incubate on a shaker for 15 minutes. The cells were blocked by adding 300 µL of blocking buffer and left on the shaker for 45 minutes. 300 µL of primary antibody (Table B2 of the Appendix) diluted in PBS-T with 10% blocking buffer was added to each well and the cells were left on a shaker overnight at 4°C.

The following day the cells were washed 3 times with 300 µL PBS. 300 µL of secondary antibodies (Table B2 of the Appendix) diluted in PBS-T was added and the plate was covered with a sheet of aluminum and left to incubate on the shaker at RT for 60 minutes. Next, the cells were again washed 3 times with PBS-T. Finally, 500 µL of 1X PBS was added to each well and the cells were visualized in a confocal microscope.

3.10.1 OPTIMIZATION OF ICC

Before staining, different antibodies were tested and to find the best concentrations. The antibodies tested for neuron staining were Microtubule Associated Protein 2 (MAP2), Neuronal Nuclear protein (NeuN), Neurofilament 200 (NF200) and Neuron-Specific class III beta-tubulin (TUJ1). MAP2 is a cytoskeletal protein expressed in the dendrites in neurons and is a good somatodendritic marker[29]. NeuN is a protein present in the nucleus of post-mitotic cells and is used to identify mature neurons[30]. Neurofilaments form the cytoskeleton in cells, and they are abundant in the axons of neurons. NF200 is hence also used as a neuronal marker to localize axons [31]. TUJ1 is expressed in the early stages of postmitotic neurons of the central and peripheral nervous system and has been used as a marker for early neuronal differentiation[32]–[34].

In addition, the mitochondrial markers Translocase of the outer mitochondrial membrane 20 (TOMM20), Acyl-CoA dehydrogenase very long chain (ACADVL), Acyl-CoA dehydrogenase medium chain (ACADM) and Cytochrome C oxidase Subunit 4 (COX4) were also tested.

TOMM20 is a protein in the TOM family and is a subunit translocase on the outer mitochondrial membrane [49]. ACADVL and ACADM belong to the family acyl-CoA dehydrogenases (ACADs) and associate with the mitochondrial membrane. These enzymes catalyze the mitochondrial fatty acid beta-oxidation pathway[50], [51]. COX 4 is a subunit of the enzyme cytochrome c oxidase and plays an important role for the regulation and the function of the regulation of the mitochondrial respiration. COX 4-1 is the principal isoform, and it is expressed in all tissues, while the COX4-2 isoform is mainly expressed under hypoxia or stressed conditions [52].
These antibodies were further used to stain fixed cells that had been differentiated from neurospheres.

3.11 WESTERN BLOTTING

Western blotting is a technique used to identify specific proteins from a mixture of proteins in cell extractions. This method identifies and separate proteins based on their molecular weight through electrophoresis. These are then transferred to a hydrophobic membrane and incubated with antibodies which are specific for the protein of interest. This should only give one band per antibody and the thickness of the band indicate the amount of protein present [35]

Prior to the blotting, protein extraction is needed to collect all the proteins in the cell cytosol. This step is done in cold temperatures and with protease and phosphatase inhibitors to prevent the denaturation of the proteins. Sonication is often needed to extract all proteins in the tissue. Then the concentration of the extraction is measured to ensure that all samples are compared on an equivalent basis.

After this the samples were ready for the SDS polyacrylamide-gel electrophoresis (SDS PAGE) in which the proteins travel through a highly cross-linked gel of polyacrylamide based on their size. The samples are put in a negatively charged solution called the loading buffer or SDS. The SDS detergent binds to the hydrophobic regions of the proteins which causes them to unfold into extended polypeptide chains[5]. The samples are also heated to denature the proteins and to ensure that their negative charge is kept so that they will migrate to the positive charge in the gel [35].

Western blotting was done on 12 samples of extracted protein from mouse brain tissue. 6 samples were from WT mice and 6 samples from KO mice, with 3 replicates from the contralateral (without HI) and 3 replicates from the ipsilateral sides (with HI) of the brain. These samples had been snap frozen 6h post HI and was kept at -80°C until protein isolation.

3.11.1 Protein extraction

900 µL of lysis buffer was made by with 90 µL Ripa lysis buffer, 9 µL of 100X protease and phosphatase inhibitor and 801 µL of MilliQ water. 200 µL of lysis buffer was added to each sample and they were sonicated for 20 seconds at 20% amplitude until properly disassociated. They were then centrifuged for 15 min at 4°C and 1000x g. The supernatant was collected.

3.11.2 Protein quantification and SDS polyacrylamide-gel electrophoresis (SDS PAGE)

Protein quantification was performed with Nanodrop with 3 replicates per sample. The average of these values was taken and used to calculate the volume of tissue needed to make a 1:4 concentration with the SDS buffer and MilliQ water.
The samples were heated at 95°C for 5 minutes. The gels were then assembled and 5 µL of sample and 2 µL of ladder was pipetted into the wells. The gel was run at 200V for 30-40 minutes. Then, the gel was transferred into a membrane in a trans-blot turbo.

3.11.3 WESTERN BLOTTING

The membrane was cut and blocked for 1 hour in 5% milk PBS-T at room temperature and left on a roller. The membranes were then incubated at 4 °C overnight with the primary antibodies (see table B3 in the appendix) in 5% milk PBS-T. The next day, the tubes were washed with PBS-T for 5 minutes, then 10 minutes and lastly 30 minutes at room temperature on a rolling incubator. Then, the samples were incubated with secondary antibodies diluted 1:20 000 in 5% milk-PBS-T. The gels were washed with PBS-T 3x 10 minutes with PBS-T, and lastly visualized with a Bio-rad ChemiDoc MP system.

3.12 LASER SCANNING CONFOCAL MICROSCOPY

Confocal scanning microscopy was invented by Marvin Minsky in 1955[36]While the conventional fluorescent microscopy illuminates the whole specimen, confocal microscopy sends a focused laser beam on a single point in a specific depth of the tissue and this has the advantage of blocking out-of-focus light, creating high-resolution 3D images [37]. With this method, only the light emitted from the focal plane is recorded by the detector and all the other background is blocked by the pinhole situated in front of the detector. In addition, scanning mirrors allows the laser beam to travel across the specimen, creating an image point by point from multiple optical sections [38].

In this study a Zeiss LSM700 confocal microscope was used to take images of the IHC stained sections. For the HI experiment, 4 images were taken by section with a 40X oil objective. 2 images were taken on the ipsilateral side, in the peri-infarct zone and the cortex and 2 on the contralateral side in the same regions. The images were captured in a z-stack of 3 images. For the lactate experiment, the images were taken with a 64X oil objective to get a closer look at the individual cells.

3.13: DATA ANALYSIS AND STATISTICAL METHODS

3.13.1: DATA ANALYSIS WAS DONE IN IMAGEJ

All images were processed and analyzed in ImageJ; an open-source image processing program developed by the National Institute of Health [39].

ImageJ was used for both the cell quantification of mature neurons and for measurement of the mitochondria in neuronal axons and dendrites. The images were blinded by a fellow laboratory member before analysis, to avoid bias during the quantification. For the quantification of mature neurons, the Z-stacks were processed with maximum intensity and then thresholded manually to create a binary image. All cells were then counted automatically with the "Analyze particles" function and the threshold was further adjusted if not all the cells were counted. Mature neurons which were NeuN+ were counted manually using the Cell Counter plugin.

For the quantification of mitochondria, the images from the Z-stack were processed with average intensity as the TOMM20 staining was strong. Then, a mask was made from the TUJ1 channel by thresholding manually and then using the "Create Mask" function (mask shown in figure 3). Furthermore, a stack of the finished mask and the TOMM20 channel was created using the "Image Calculator" function and the operation "AND". This image was again thresholded and the mitochondria that are both TUJ1+ and TOMM20+ were counted manually using the ROI manager.

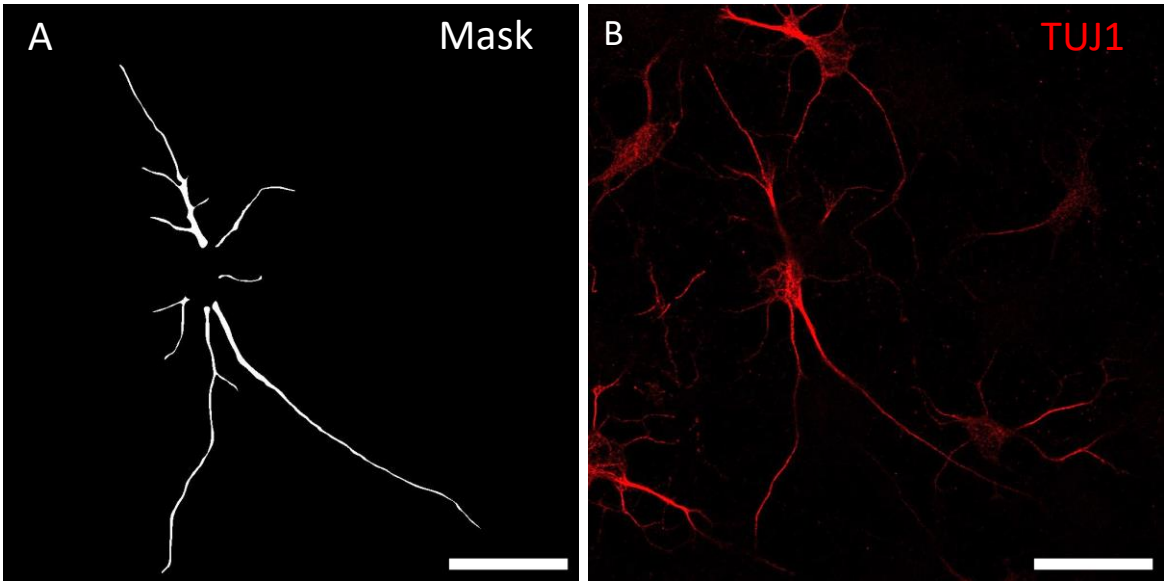

Figure 5: Example of a mask created from the TUJ+ channel using the "Image Calculator" function. Mask (A) generated from the TUJ channel (B). Scale bar: 30 μm.

.

3.13.2: STATISTICS

During the analysis of the blinded images, all the data was recorded into Microsoft Excel. When all the images were analyzed, the groups were unblinded and organized into tables. This data was then transferred to GraphPad Prism in which statistical analysis and the generation of graphs was performed.

Different statistical analyses were made for each experiment. For the HI experiment, a two-way ANOVA test was performed with Šidák correction for multiple comparisons. The mean value was presented with the standard deviation (SD) and a p-value of 0,05 with a confidence interval of 95% was used. For the second experiment, an unpaired t test was performed to see if there was a significant difference in the size and number of the mitochondria in two independent groups, with a two-tailed p-value. Repeated measures ANOVA cannot handle missing values, and as one of the values from the western blot was missing, the data for the last experiment was analysed using a mixed effects model.

4. Results

4.1 Survival of mature neurons after induced hypoxia-ischemia

4.1.2 Immunohistochemistry

To test whether HCAR1 affects the survival of mature neurons after HI, we immunolabeled and quantified mature neurons in brain sections from mice that had undergone HI. Several markers exist for mature neurons. To determine the best antibodies and antibody concentration for our experiments, we first performed preliminary testing and optimization (see concentrations in table B1 of the Appendix). The neuronal markers tested were MAP2 and NeuN. Since the quantity of cells after HI can reflect the number of cells that survived HI as well as newly proliferated cells, we also included the proliferation marker BrdU. Overlap between BrdU+ and NeuN+ cells would indicate proliferating cells that had later differentiated into mature neurons.

NeuN gave a strong staining with minimal background noise, as shown in Figure 6C and Figure 7B. The MAP2 staining was also strong, but the microfilaments appeared too dense and meshed for further analysis. Although MAP2 also labels neuronal cell bodies, this labeling was weaker and would be less reliable for quantitative analysis than NeuN (Fig. 6B and 7C). Some BrdU+ cells were found, but none of them overlapped with NeuN (Fig. 6D-E and 7D-E). This suggests that no proliferating neuronal progenitors had time to mature into neurons before the mice were sacrificed. Therefore, the NeuN+ cells reflect neurons that survived the HI and not new neurons. Hence, BrdU was not further used in the main experiment.

With these results, DAPI and NeuN were the antibodies chosen for the main experiment. IHC was performed on 10 coronal brain sections, 5 from WT and 5 from KO. These were from 16 days old mice that had undergone HI at 9 days of age.

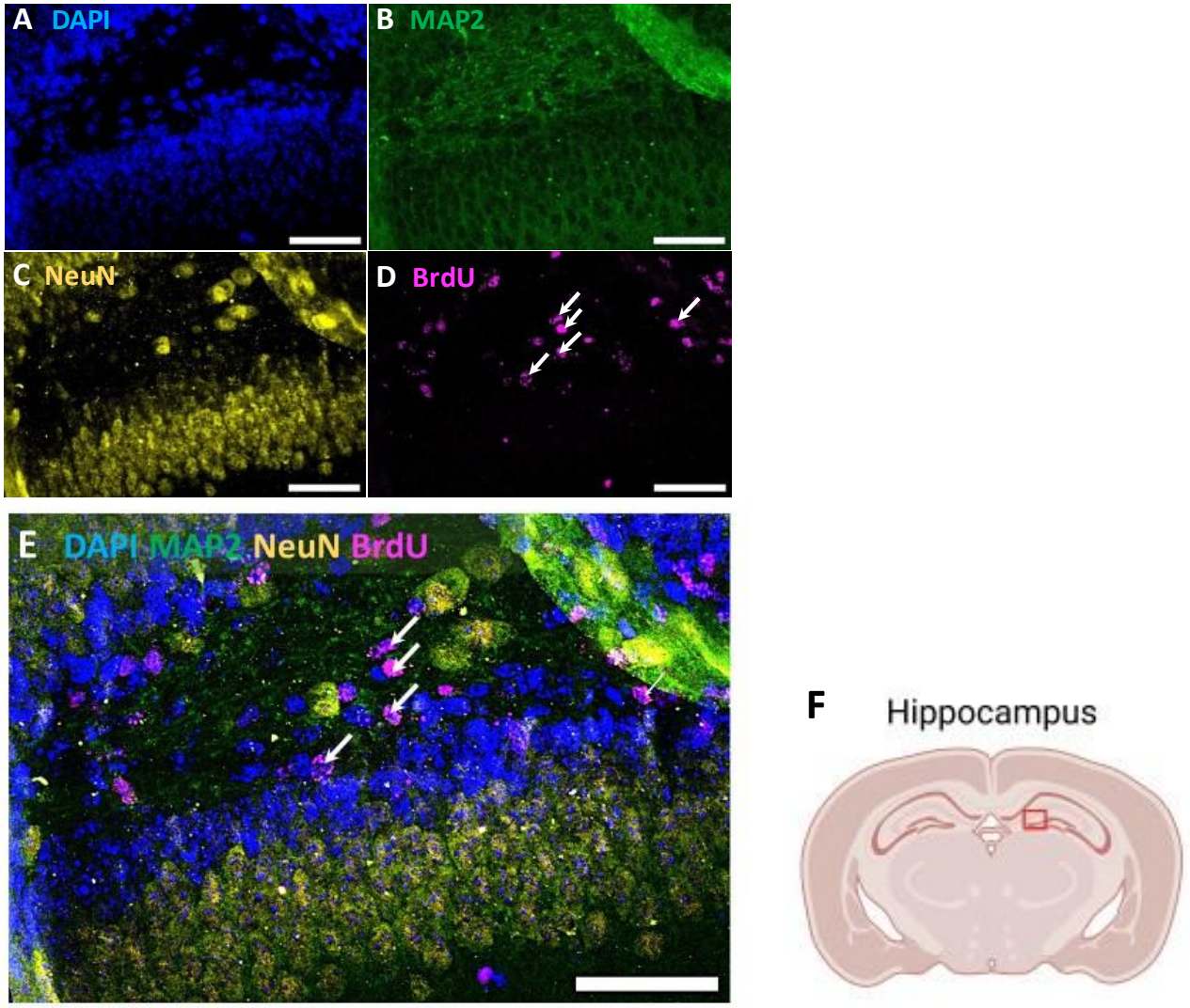

Figure 6: Optimization experiment for staining of mature neurons after induced HI.

A-D: Confocal images from the hilus of the hippocampus in a coronal brain section from a WT mouse. The sections are labelled with DAPI (all nuclei, **A**), MAP2 (neuronal dendrites and cell bodies, **B**), NeuN (Neuronal nuclei, **C**) and BrdU (nuclei of proliferating cells, **D**).

E: Merged image with DAPI, MAP2, NeuN and BrdU.

F: Figure showing the hippocampus and the localization this image was taken. Figure made in BioRender

White arrows: DAPI+ BrdU+ cells. Scale bar: 50 μm.

.

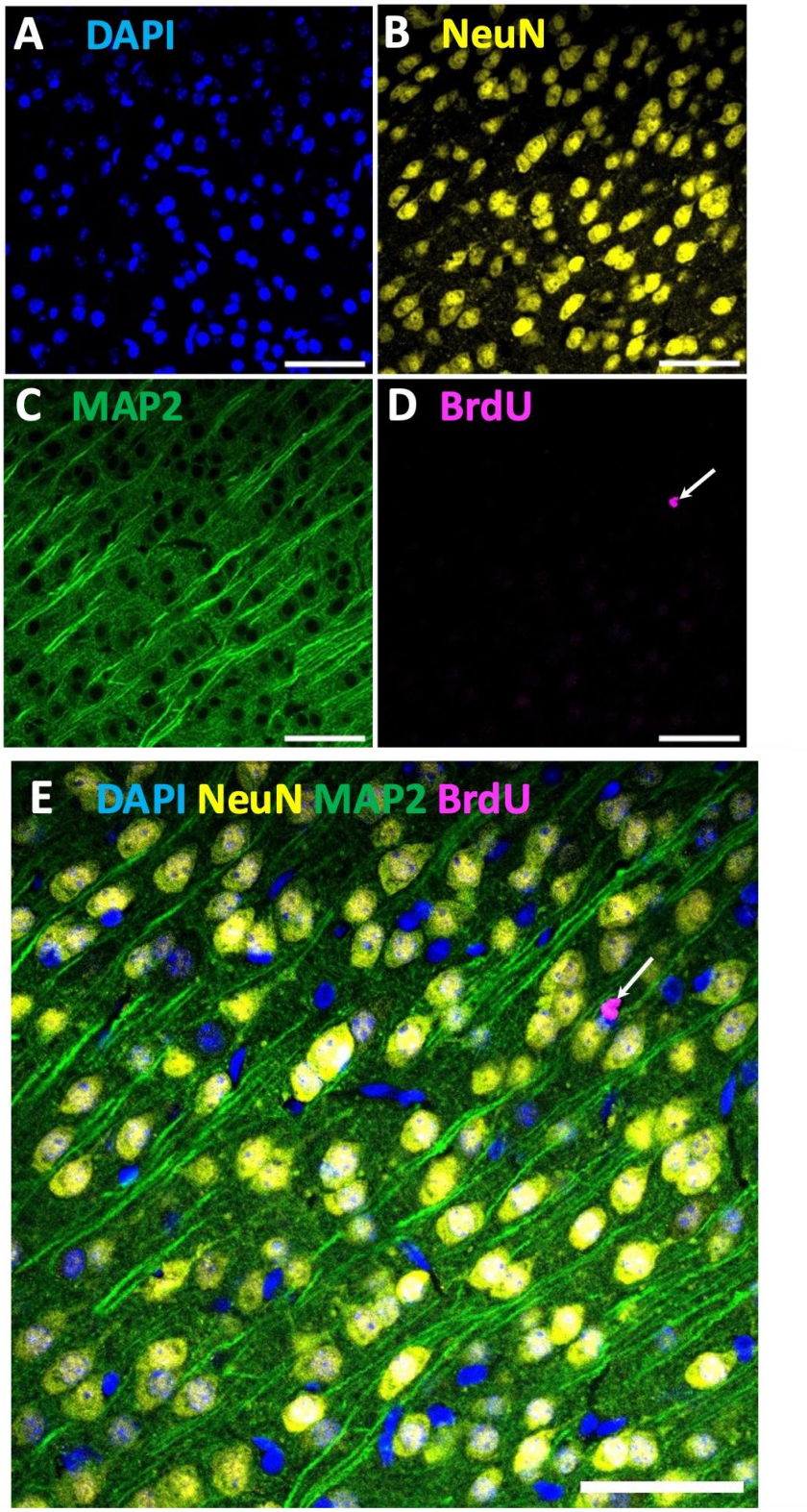

Figure 7: Optimization experiment for staining of mature neurons after induced HI.

A-D: Confocal images taken close to the lateral ventricle of coronal brain sections of WT mice. The sections are labelled with DAPI (all nuclei, **A**), MAP2 (neuronal dendrites, **B**), NeuN (Neuronal nuclei, **C**) and BrdU (Proliferating neurons, **D**).

E: Merged image with DAPI, MAP2, NeuN and BrdU. White arrows: DAPI+ BrdU+ cells. Scale bar: 50 μm.

4.1.3 Quantification of mature neurons in the peri-infarct zone

We first wanted to quantify the density of neurons in the peri-infarct zone. This is the area adjacent to the ischemic core of the infarct. We quantified neurons in the peri-infarct area, medial to the ischemic core on the ipsilateral side, and in the same area on the contralateral side (Figure 8, H). The results are shown in Figure 8.

First, the total cell density (DAPI+ cells/area) was calculated to get a measure of the total change in the cell population. There was no significant difference between the ipsilateral and the contralateral hemispheres in WT mice (Figure 8, F, DAPI/0,01mm^2: contra: 18.,45 ± 3,42, ipsi: 2,10 ± 4,00, p= 0,38, df=8,00, n=5). Similar results were found for the cell density in KO mice (Figure 8, F, DAPI/0,01mm^2, contra: 19,84 ± 1.28, ipsi: 22,98 ± 1,91, p= 0,28, df= 8,00, n=5).

We then quantified mature neurons (NeuN+ cells). In WT mice, there was no significant difference in the density of mature neurons between the contralateral and ipsilateral side (Figure 8, G, WT; NeuN+/0,01mm^2; contra: 10,18± 2.52, ipsi: 8,45± 4,02, p= 0,64, df= 8,00, n=5). In KO mice, however there was a significant increase of mature neurons on the contralateral side compared to ipsilateral (Figure 8, G, NeuN+/0,01mm^2; contra: 14,40 ± 1,64, ipsi: 8,48± 4,19, p= 0.033, df= 8,00, n=5). The cell ratio of NeuN+ cells to total cells (NeuN+ cells / DAPI+ nuclei) was also calculated and showed a similar trend as the NeuN+ density analysis. There was no significant difference in the cell ratio of NeuN+ cells for the WT mice (Figure 8, H, %NeuN/DAPI+cells, contra: 57,29±9.63±%, ipsi: 43,17±23,27%). However, the KO mice showed a significant increase in the ratio of mature neurons on the contra side compared to the ipsi side (Figure 8, H, %NeuN/DAPI+cells, contra: 73,33±11,48%, ipsi: 39,14±14,21%).

Thus, these data indicate that mature neurons in HCAR1 KO mice have lower survival after HI than mature neurons in WT mice. However, though the KO mice have a higher loss of neurons after HI, their average density of neurons on the contralateral side seems higher than in WT mice (Figure 8, I, NeuN+/0,01mm^2, WT, contra= 10,17±2,25, KO, contra=14,39±1,64, p=0,017, n=5). Therefore, despite the higher loss of neurons in KO, the average density of neurons after HI seems relatively similar between KO and WT.

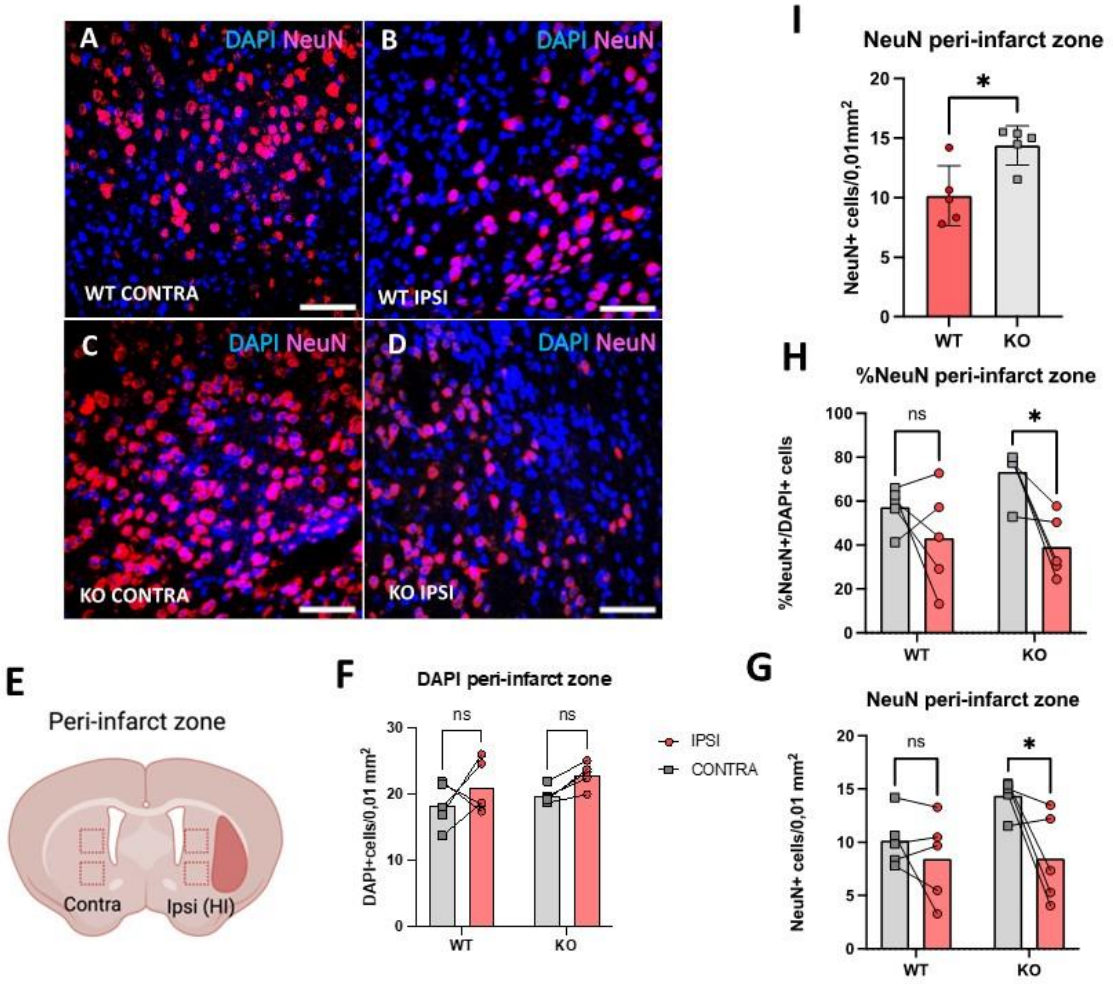

Figure 8: Quantification of mature neurons in the peri-infarct zone

A-D: Confocal images of NeuN+ cells/area in the peri-infarct zone from the contralateral (A, C) and the ipsilateral hemisphere (B, D). Scale bar = 60 µm.

E: Figure of a coronal mouse brain section indicating the areas where the images were captured (red squares). The injury caused by HI is indicated by the red region on the ipsi side.

F-I: Analysis of cell density (DAPI+ cells/ 0,01 mm^2, F) , the density of mature neurons (NeuN+ cells/ 0,01 mm^2, G) and the ratio of mature neurons to all other cells (%NeuN+/DAPI+ cell, H) in the ipsilateral (pink bar) and the contralateral (grey bar) hemispheres.) The density of mature neurons in the contra side of KO and WT has been additionally analyzed (NeuN+ cells/ 0,01 mm^2, I). *p>0,05. Each point represents one mouse, and the ipsilateral and contralateral hemispheres of the same mouse is connected by a line. WT and KO n=5. The p-values were calculated using the Sidak method.

The data points in E-G represent the average value from the two images on either the contra- or ipsilateral hemisphere. Figure made in BioRender.

4.1.4 QUANTIFICATION OF MATURE NEURONS IN THE CORTEX

The survival of mature neurons was also studied in the cortex, which is located further away from the ischemic core (Figure 9, H).

Similarly to the study of the peri-infarct zone, the overall cell density (DAPI+cells/area) was analyzed in the cortex but no significant difference was found between the two brain hemispheres in the WT mice (Figure 9, F, DAPI+/0,01 mm^2; contra=16,33±2.96, ipsi= 18,00±3,98, p= 0,51, df= 8,00, n=5) and the KO mice (Figure 9, F, DAPI+/0,01mm^2, contra= 16,99±6.22, ipsi: 17,75±5,34, p= 0,86, df= 8,00, n=5).
No significant difference was found for the quantification of the NeuN cell density (NeuN+ cells/area in WT mice (Figure 9, G, NeuN/0,01 mm^2, contra: 10,33±2,89, ipsi: 11,34±2,95, p= 0,74, df= 8,00, n=5). This was also the case for the KO mice (Figure 9, G, NeuN/0,01mm^2, contra: 11,57±5,14, ipsi: 9,80±3,54, p= 0,42, df= 8,00, n= 5).
Furthermore, the quantification of the NeuN cell ratio (%NeuN+ cells/DAPI+ cells) don't show any significant difference for the WT mice (Figure 9, H, %NeuN+ cells/DAPI+ cells, contra: 65,87±12.65 %, ipsi: 63,18±10,61%, p= 0,91, df= 8,00, n=5) or the KO mice (Figure 9, H, %NeuN+ cells/DAPI+ cells, contra: 66,54±21,50%, ipsi: 59,19±11,51±%, p= 0,52, df= 8,00, n=5). Lastly, there was no significant difference between the density of mature neurons between the WT and the KO mice (Figure 9, I, WT, contra= 10,33±2,89, KO, contra= 11,57±5,14, p=0,65, n=5).

These data indicate that HI does not lead to significant loss of neurons in areas of the neocortex that are further away from the ischemic core than a typical peri-infarct zone. They further indicate that HCAR1 does not influence the neuronal density in these areas.

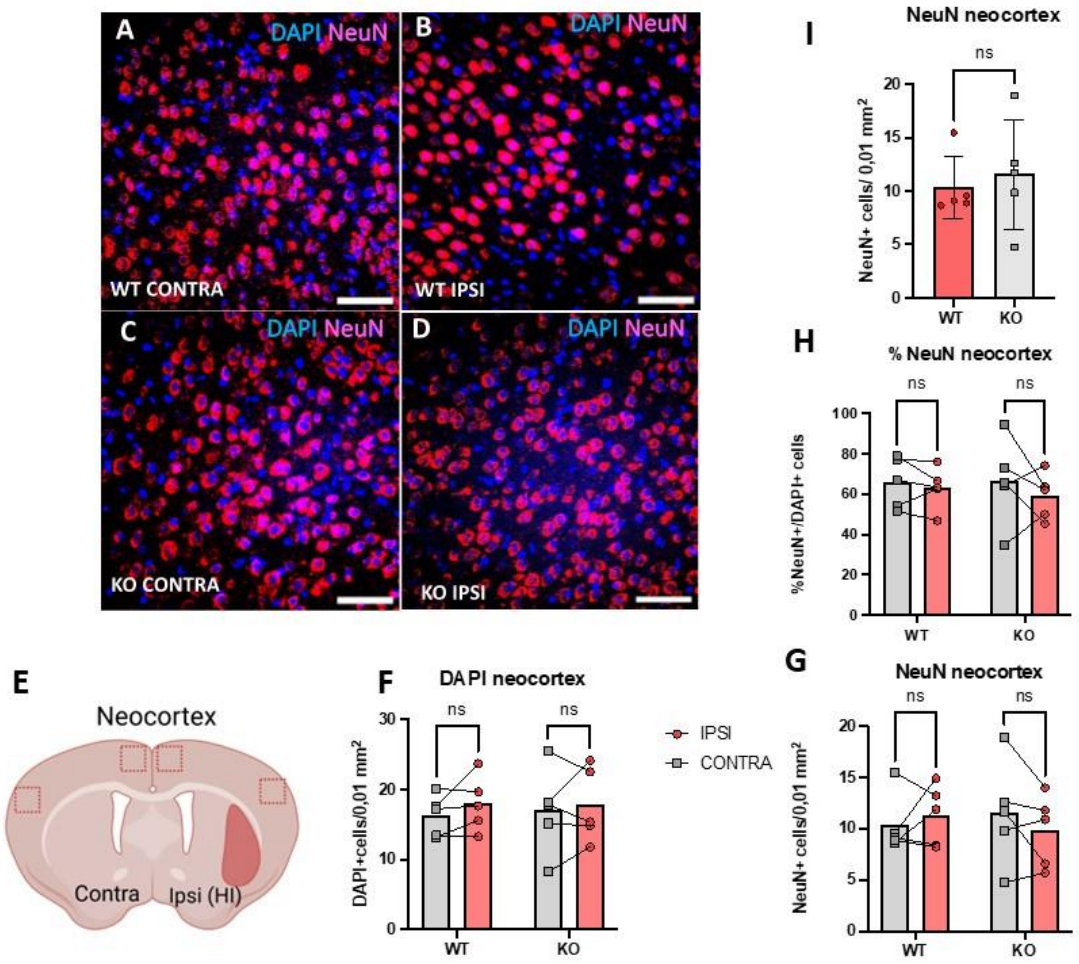

Figure 9: Quantification of mature neurons in the neocortex

A-D: Confocal images of NeuN+ cells/area in the peri-infarct zone from the contralateral (A, C) and the ipsilateral hemisphere (B, D).

E: Figure of a coronal mouse brain section indicating the areas where the images were captured (red squares). The injury caused by HI is indicated by the red region on the ipsi side. Created in BioRender.

F-I: Analysis of cell density (DAPI+ cells/ 0,01 mm^2, F), the density of mature neurons (NeuN+ cells/ 0,01 mm^2, G) and the ratio of mature neurons to all other cells (%NeuN+/DAPI+ cells, H) in the ipsilateral (pink bar) and the contralateral (grey bar) hemispheres). The density of mature neurons in the contra side of KO and WT has been additionally analyzed (NeuN+ cells/ 0,01 mm^2, I). *p>0,05. Each point represents one mouse, and the ipsilateral and contralateral hemispheres of the same mouse is connected by a line. WT and KO n=5. The p-values were calculated using the Sidak method. Scale bar = 60 µm.

4.2 THE EFFECT OF LACTATE ON NEURONAL MITOCHONDRIA

To test whether lactate can influence the density of mitochondria in neurons, we treated differentiated neurospheres with lactate and then quantified the neuronal mitochondria with immunocytochemistry.

4.2.1 OPTIMIZATION OF ICC

To visualize the mitochondria in the cell, preliminary testing of the antibodies was performed to find the most suitable mitochondrial and neuronal marker. The mitochondrial markers COX4, ACADM, ACADVL and TOMM20 were tested together with the neural marker TUJ1 and the axonal marker NF200 (Table B2 in the Appendix).

Figure 7 shows the staining of ACADM (Figure 10, C) and ACADVL (Figure 10, G). ACADM gave a relatively good staining, but ACADVL seemed to be a little weak in comparison. Both COX4 and TOMM20 gave a strong staining (Figure 11, C, G). TOMM20 seemed to be the best mitochondrial marker as it gave strong staining at low concentrations and with minimal background noise. However, TOMM20 cannot be used in combination with MAP2 as both come from the same host animal and this can lead to the secondary antibodies cross-reacting with each of the primary antibodies[57]. As TUJ1 comes from a different host animal, it was chosen as the neuronal marker in combination with mitochondrial marker TOMM20 for the main experiment. We did observe some axons that were positive for NF200 (not shown), but overall there were few NF200 positive axons. NF200 is typically expressed in medium-large diameter axons, which there may have been few of in our preparation[58]. Therefore, NF200 was not suited to identify axons in our neurospheres.

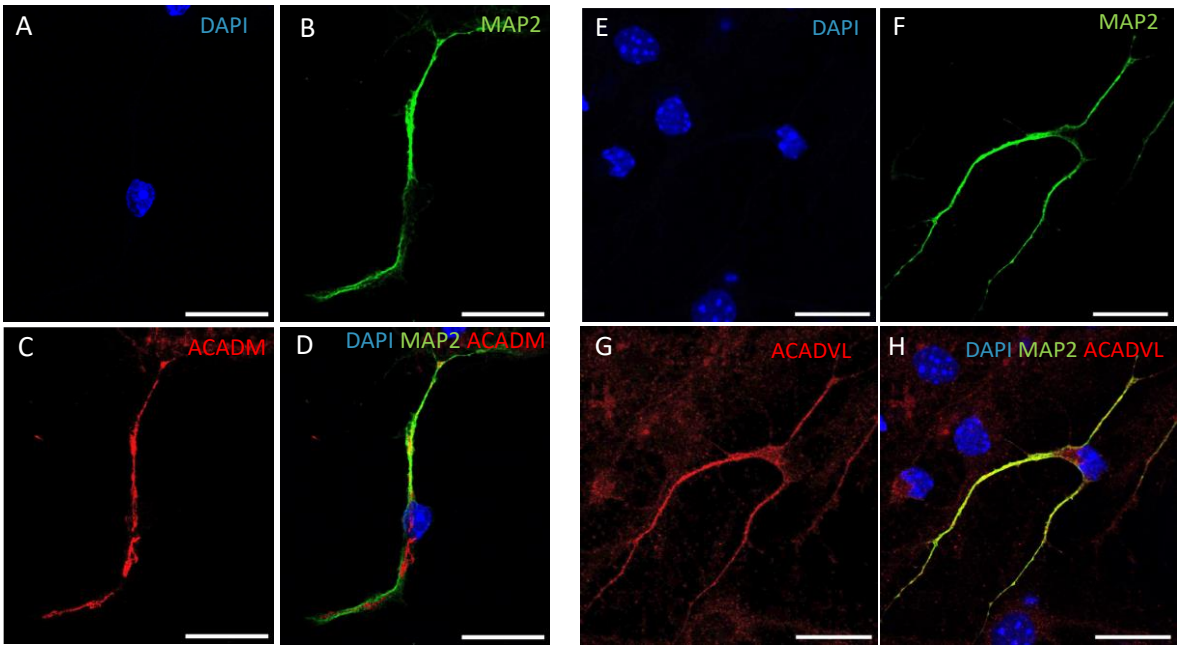

Figure 10: Testing of mitochondrial and neuronal markers for ICC on differentiated neurospheres.

A-D: Confocal image of a neuron on a slide with differentiated neurospheres stained with DAPI (A), MAP2 (B), ACADM (C) and the merged image of DAPI, MAP2 and ACADM (D).

E-H: Confocal image of a neuron on a slide with differentiated neurospheres stained with DAPI (E), MAP2 (F), ACADVL (G) and merged image of DAPI, MAP2 and ACADVL (H).

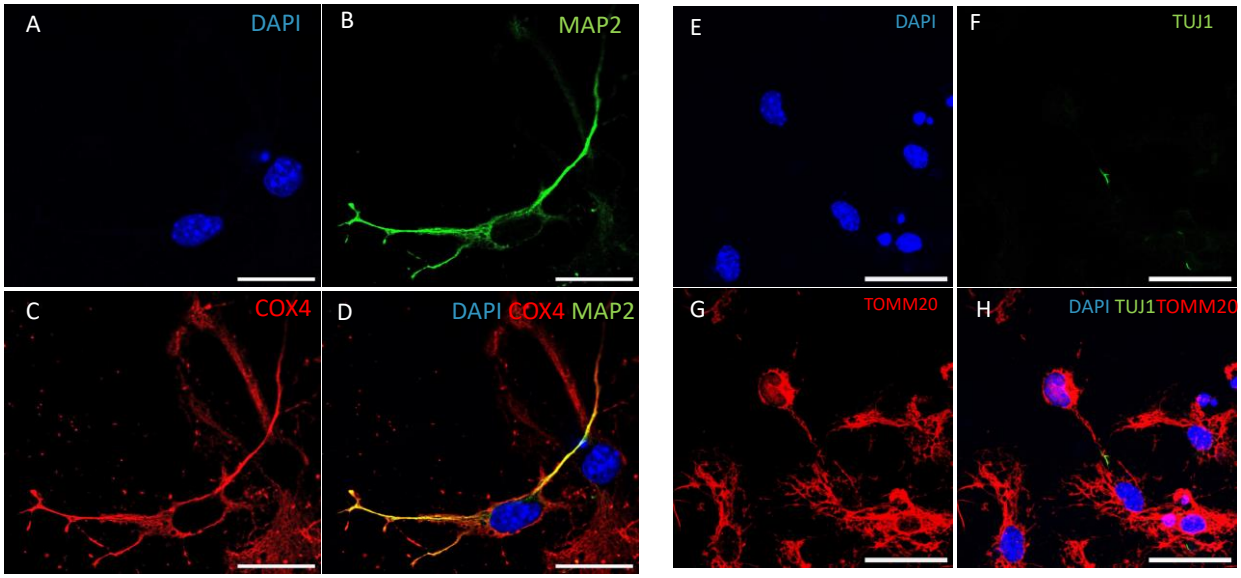

Figure 11: Testing of mitochondrial and neuronal markers for ICC on differentiated neurospheres.

A-D: Confocal image of a neuron on a slide with differentiated neurospheres stained with DAPI (A), MAP2 (B), COX4 (C) and the merged image of DAPI, MAP2 and COX4 (D).

E-H: Confocal image of a neuron on a slide with differentiated neurospheres stained with DAPI (E), TUJ1 (F), TOMM20 (G) and merged image of DAPI, TUJ1 and TOMM20 (H).

4.2.2 THE EFFECT OF LACTATE ON MITOCHONDRIAL SIZE AND DENSITY

To study the effect of lactate on the mitochondria in neurons treated with and without lactate, five different analyses were done. In all the analyses described below, we excluded the cell body, since the high density of mitochondria there make it hard to quantify. Therefore, the analyses were focused on dendrites and axons.

First, the total area of TUJ1 was measured to obtain the area of the axons and dendrites of every cell. This is a useful to see if there are any significant differences in the axonal and dendritic size between the WT and KO mice. The total area of TUJ1 was shown to be very similar in the treated and control cells and no significant change was found (Figure 12, I, Area TUJ1(mm^2), control: 349,9±166,2, treated= 405,4±263,4, p= 0,58, df= 18, n=10).
Then, the total area of TOMM20 was measured (Figure 12, J). The total area of TOMM20 measures the area of all the mitochondria present in the axons and the dendrites in each cell and gives an indication of the total area covered by mitochondria in the cell. It was calculated by summarizing all the areas of all the mitochondria in the cell. No significant difference was found in the treated versus control cells (Figure 12, J, TOMM20(mm^2), control= 190,3±100,8, treated= 193,6±131,2, p= 0,95, df=18, n=10).
Since the size of individual mitochondria can reflect their respiration status (cells with large, elongated mitochondria have higher respiration than cells with lots of small, fractionated mitochondria), we then measured **the average area of individual mitochondria** (Figure 12, K). This analysis did not show a significant difference between the treated and the control cells (Figure 12,K, average TOMM20 area (mm^2), control= 5,57±1,74 treated= 5,18±1,49, p= 0,59, df=18, n=10).
The ratio of %TOMM20/TUJ1 measures the percentage are covered by mitochondria. No significant difference was found in this study (Figure 12, L, %TOMM20/TUJ1, control: 54,78±8,72, treated= 50,45±17,53, p= 0,49, df= 18, n=10).
Lastly, the number of mitochondria was also quantified as this is an interesting parameter to study the possible effect that lactate can have on the mitochondria. However, the results did not show a significant change (Figure 12, M, control= 36,40±17,44, treated= 38,40±21.58, p= 0,82 ,df= 18, n=10).

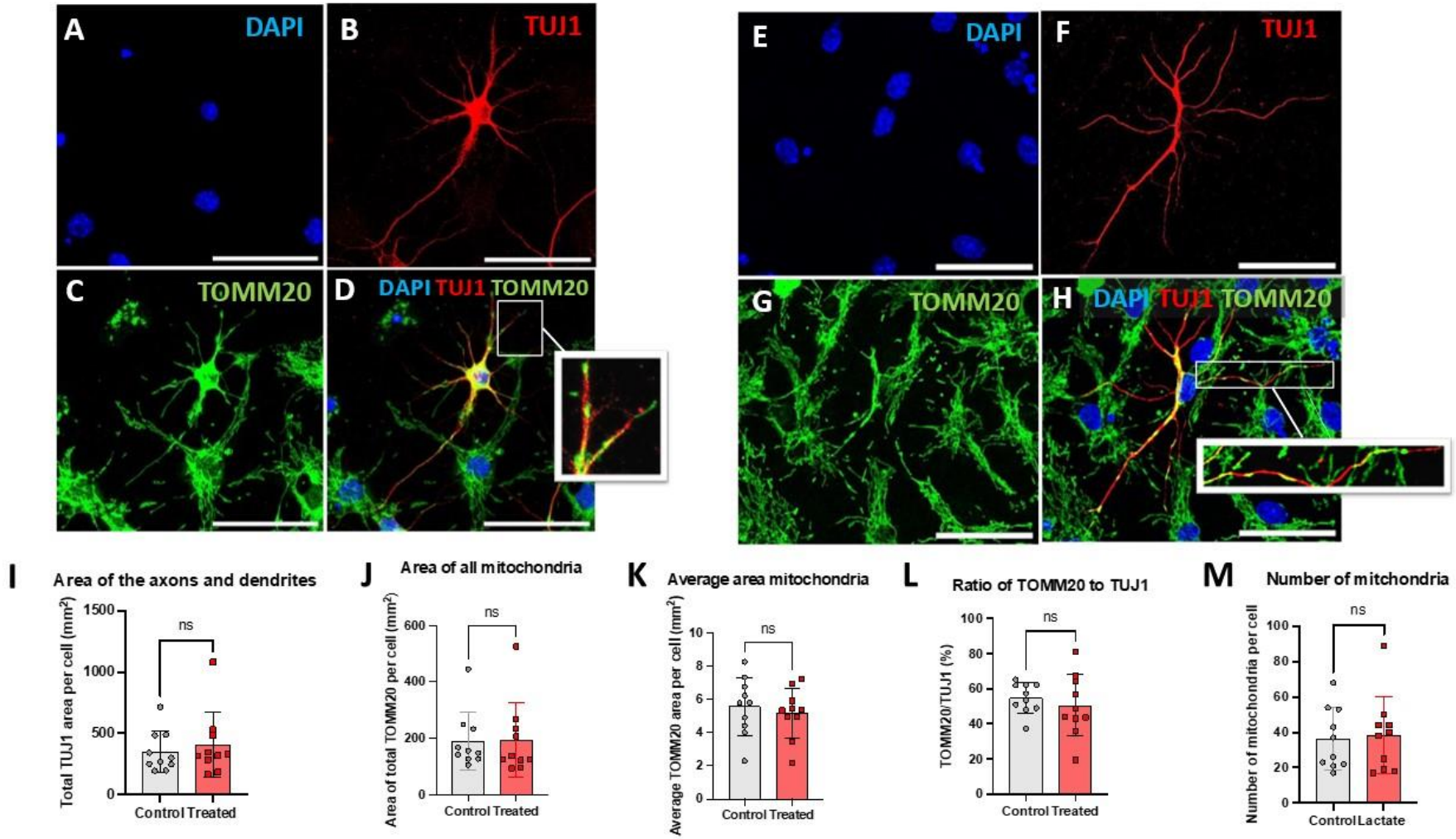

Figure 12: The effect of lactate on mitochondrial dynamics in control cells and cells treated with lactate.

A-H: Confocal images of a control cell (A-D) and a cell treated with lactate (E-H). The cells are immunostained with DAPI (all cell nuclei, blue, A, E), TUJ1 (neuronal axon and dendrites, red, B, F), TOMM20 (mitochondria, green, C, G) and the merged image with DAPI, TUJ1 and TOMM20 (D, H). An insert was made to show the individual mitochondria in the dendrites. Scale bar = 40 µm.

I-M: Analyses of the total area of TUJ1 in control and treated cells(I), the area of all the mitochondria per cell (mm^2) (J), the average area of the mitochondria per cell (mm^2) (K), the ratio of TOMM20 to TUJ1(L) and the number of mitochondria per cell (M). Each point represents one cell, with treated cells shown in the pink bar and control cells in the grey bar. Error bars= SD and n=10.

4.3 Protein analysis of mitochondria in WT and KO mice with HI

To further investigate the effect of HCAR1 on the mitochondria, protein levels of COX4 and TOMM20 were measured in P9 KO and WT mice with induced HI through western blotting. 12 samples were analyzed in total, 6 samples from KO mice and 6 from WT mice with 3 samples from each brain hemisphere (ipsi and contra). The blot is presented below (Figure 13, A). COX4 showed a band at around 17 kDa. An air bubble appeared on the band of WT1 during the transfer from the gel to the membrane and it has hence done been excluded from the graphs. A mixed-effects analysis was performed in which is similar to the previous ANOVA test of repeated measures but allows for missing values. This test showed that the expression of COX4 was significantly higher in WT mice compared to the KO mice and that this was significant on the ipsi side (Figure 13, B, WT, ipsi= 1,96±0,27, KO, ipsi= 0,95±0,51, p= 0,04, n=2). However, since WT only had 2 datapoints this can only show a trend. This trend was also observed on the contra side ((Figure 13, B, WT, contra= 1,88±0,22, KO= 1,043±0,38, p=0,06, n= 3).

TOMM20 gave a clear band at around 16kDa (Figure 13, A). However, the expression of TOMM20 relative to vinculin did not show a significant difference between WT and KO mice on the ipsi side (Figure 13, C, WT, ipsi: 5.26±0,61, KO, ipsi= 7,28±2,87, p= 0,52, n=3), nor on the the contra side (Figure 13, C, WT, contra= 7.99±3.40, KO, contra= 6.44±2.03, p= 0,66, n=2).

This experiment could indicate that HCAR1 would not affect TOMM20 after 6 hours of HI, but that there might be a trend of COX4 being underexpressed in the HCAR1 KO mice.

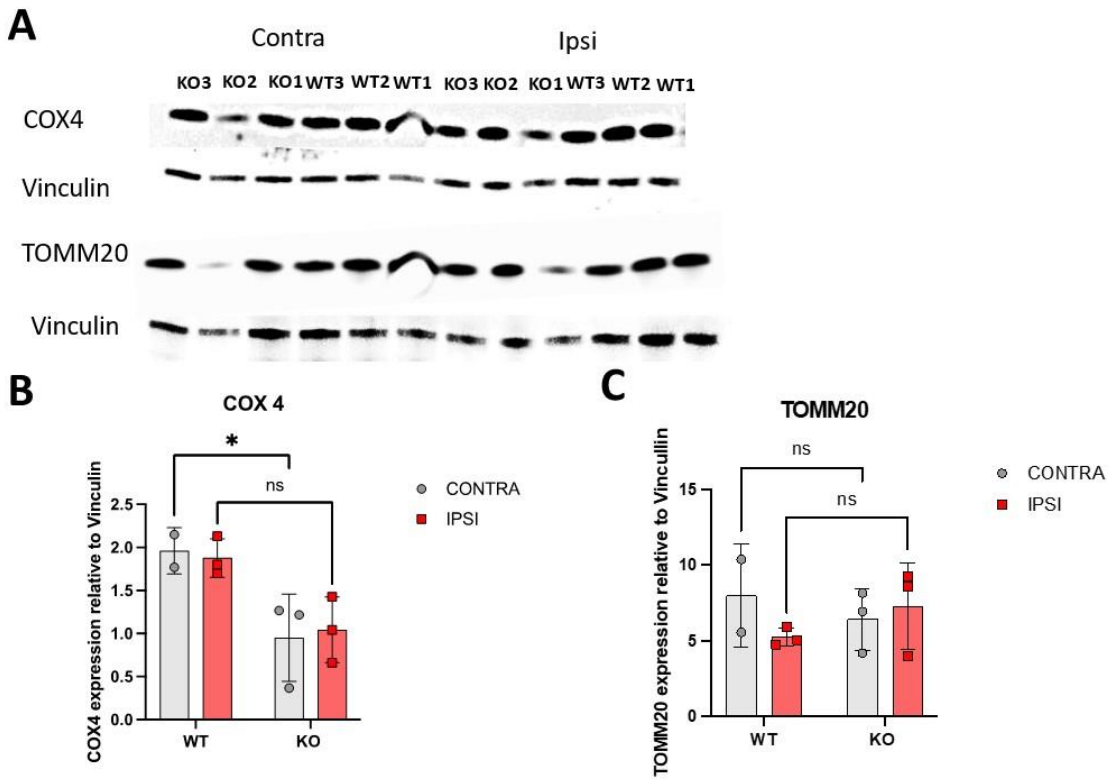

Figure 13: COX4 and TOMM20 protein expression in WT and HCAR1 KO mice.

A: Western blot of brain tissue samples from P9 WT and KO mice 6 hours post HI. The left side of the membrane show the contra side of the brain while the right side of the membrane represents the ipsilateral and contralateral hemispheres. COX4 and TOMM20 gave a strong band at 17 and 16 kDa. Vinculin was used as the housekeeping protein.

B: COX4 expression relative to vinculin in the ipsi and contra sides of the brain of WT and KO mice.

C: TOMM20 expression relative to vinculin in the ipsi and contra sides of the brain of WT and KO mice. Every point represents one mouse. Error bar=SD, n=3.

5. Discussion

This section will first present this project's initial planned experiments and the experimental changes that were made. Then, the methods used as well as the potential changes that could have been made to give better results will be discussed. Lastly all results will also be presented and discussed as well as future perspectives.

5.1 Initial experiments and changes

The initial overall aim of this project included studying the effect of lactate on mitochondrial movement in neurons and the possible role of the lactate receptor HCAR1. This aim would have included the live imaging microscopy of neurons. However, after several months of problems with the proliferation and differentiation of the neurospheres, another aim was added involving studying the survival of mature neurons after HI on mice with the HCAR1 gene (WT mice) and the mice lacking the HCAR1 gene (KO mice). This research was based on our group's latest paper in which we found that lactate improved recovery after HI and the regeneration of brain tissue through the activation of HCAR1, which stimulates neurogenesis. In this paper, they focused on the receptor's role in the survival of proliferating neurons while this thesis focuses on the survival of mature neurons.

After this analysis and extensive troubleshooting, 2 plates of neurospheres were at last successfully differentiated, treated with lactate and stained to study the effect of lactate on mitochondrial size and density in the axons and dendrites of fixated neurons.

5.2 DISCUSSION ON METHODS

A range of different laboratory techniques were done under this study. Most of this project was spent on the optimalization of techniques, IHC and ICC experiments as well as image analysis.

5.2.1 NEUROSPHERES

Benefits of neurospheres

Since its description by Reynolds and Weiss in 1992, neurospheres have been a powerful model to study neurons and neurogenesis in vitro due to their capacity to self-renew, proliferate, and differentiate into different mature cell types. These are very important processes during embryonic brain development but also for tissue regeneration in the adult brain [33].

There are many advantages with using neurospheres as a model system. First, it is a method which gives rise to a source of undifferentiated cells which can be further expanded into culture. These cells can be tested for a range of different conditions in a controlled environment[33]. Another advantage of the neurospheres compared to other methods is the reduction in the number of mice needed per experiment, a high number of cells can be isolated per mouse[33]. In this study, we only used cells that had been differentiated from neurospheres. The big advantage of this method has been to be able to study individual cells without disturbances from surrounding brain tissue as well as being able to treating the cells with a controlled amount of lactate. As an alternative, it would have been possible to perform the experiments on organotypic brain slices, but mitochondrial imaging is much easier in the neurospheres since the cells lay on a flat coverslip instead of the three dimensional space of a brain slice.

Limitations of the neurospheres

Although there are numerous advantages with the neurospheres, there are also limitations with this method. The neurospheres are highly dependent on variables such as age, seeding density, culturing conditions and the number of passages to proliferate and differentiate. Problems with the proliferation and the differentiation with the neurospheres lead to some troubleshooting which can be difficult as the neurospheres are also very dependent on the many steps reagents and on the many steps of the protocol such as the dissection process, the disassociation, and the components present in the medium [33]. Another, obvious limitation of using differentiated neurospheres is that this is an artificial system where the cells are isolated from their natural environment. The differentiated neurons studied in this thesis were plated with relatively sparse density on coverslips and presumably had fewer synaptic connections than they would have had in an intact brain. This can of course influence the results.

5.2.2. MOUSE MODEL FOR HYPOXIA ISCHEMIA AND GENETIC KNOCK-OUT OF HCAR1

Most of our knowledge about pathophysiological mechanisms of brain diseases come from studying animal models, and they are an essential tool for studying hypoxia-ischemia. There are many advantages which come with using smaller animals, such as mice, to study hypoxia-ischemia. Compared with larger mammals, they are less expensive and easier to genetically modify. Importantly, they are also being considered more ethically acceptable for animal experiments [59], [60]. Rodents have similar cerebrovascular anatomy and pathophysiology as humans, however there are also several differences. They have smaller brains than humans, the structure and the length of perforating arteries is different and the ratio of grey to white matter is lower in humans. Although they have some resemblances, HI is a heterogenous condition an no animal model can completely mimic the complexities of the human stroke [60].

In this study, the Levine method was used to induce HI in HCAR1 KO and WT mice [61]. An advantage of using the mouse model is that it allows for studying HI in a whole organism with an intact cerebrovascular system. In addition, HI can be induced in a controlled environment as well as testing different treatments. Also, since mice have smaller brains, it makes the

evaluation of the whole brain faster and easier. However, compared to the neurospheres, in vivo studies require the termination of more animals.

5.1.3 Imaging analysis

Most of the images in this project were taken with the confocal microscope with different settings for experiment 1 and 2. For the quantification of mature neurons in brain slices with induced HI, it was preferred to get as many cells as possible per image while being able to tell individual cells apart, and a 40x oil objective was therefore used. In contrast, the images taken for the experiment testing lactate on the mitochondria were taken with a 64x oil objective to get a closer look at the individual cells and the mitochondria present in the axons and dendrites. It should be mentioned that individual mitochondria cannot always be told apart when using confocal microscopy. This is because mitochondria that lay close together will have a smaller space between them than the spatial resolution limit for confocal microscopy (around 200 µm) [55]Therefore, our estimation of mitochondrial density will be an underestimate.
Another problem that could occur under the image analysis of the IHC experiments is that the quantification could be biased. Hence, the images had to be blinded and the genotypes of the mice or the treatment of the cells were not known until the quantification was finished to prevent subjective biases that could potentially affect the data.

5.2 Discussion of the results

5.2.1 Survival of mature neurons after HI

In developed countries, hypoxia-ischemia is a condition occurring in 1,5 per 1000 infants per year and can lead to serious neurological long-term effects [32], [62]. To this day, there are no effective treatments which totally prevent these long-term effects as hypothermia is only efficient for less than 60% of babies [30]. Recent findings of our groups have shown that HCAR1 plays an active role in the regeneration of brain tissue and could be a target for future treatment of HI [32].

The first aim of this project was to look at survival of mature neurons after HI and the possible role of HCAR1.

The analysis of the cell density and ratio of mature neurons performed in this study suggests that HCAR1 plays an important role for neuron survival after hypoxia-ischemia. The quantification of NeuN+ cells per area in the peri-infarct zone in the HCAR1 KO mice showed a significantly higher number of mature cells on the contralateral side, which was not affected by HI, compared with the injured ipsilateral side. In our groups' article they measured the brain tissue loss 42 days after HI when the repair process is completed. A tissue loss of 17±9% was found in WT mice, but this loss was significantly higher for KO mice which had a 31±10% of tissue loss [32]. However, they also measured tissue loss after 24 hours but did not find a significant difference in the acute tissue loss between WT and KO mice. From this finding, they concluded that the tissue loss which was higher in KO mice after 42 days was caused by a decrease in cell proliferation and tissue regeneration. However, since my data show increased neuronal death ipsilaterally in KO, but not in WT, it is possible that the tissue loss in KO mice was also caused by neuronal cell death that occured later than 24 hours post HI. The brain slices that I analyzed were fixed 7 days after HI, which gives time for more cells to die, but not enough time for newly proliferating cells to mature to neurons (since we found no KI67 positive neurons). Neuronal cell death in the KO mice could further be investigated through IHC experiments with apoptosis markers such as caspases, or with a TUNEL assay which can detect apoptotic and necrotic cells which undergo DNA degradation.

Similarly, to what was done in our group's article, the total cell density (DAPI+ cells/area) was also quantified. Based on their findings, an increase in the overall cell density would have been expected on the ipsi side since moderate hypoxia can induce cell proliferation [32] [63]. However, no significant change was observed between the side affected by HI and the side which was not injured in both WT and KO mice. This was also the case in the cortex where the average cell densities were not only not significantly different, but almost identical. This makes sense as the peri-infarct zone is situated right next to the infarct, while the cortex is further away and is probably less affected by HI. However, there was found to be a significantly higher density of the total number of cells in the peri-infarct zone in the KO mice compared to the WT mice. This might suggest that although HCAR1 might be important to the survival of mature cells, it might not be as important other cells.

Several recent studies in mice have shown that the administration of extracellular lactate before and after HI has reduced the size of the damaged area and improved recovery [30], [31]. This protective effect is thought to be both a metabolic and a HCAR1 dependent effect, as lactate has also been replaced with a receptor agonist which also gave partial protection [64]. Hence, it is expected that additional lactate injections in the mice before or after HI would have amplified the effect of HCAR1 and possibly give a higher survival rate of mature neurons in the WT mice in this study.

Limitations in the analysis of neuron survival after HI

The increase in the total cell density and ratio of mature neurons was not significant for the WT mice, and although one might expect a more significant change for this genotype based on previous studies[32], this result could be caused by several reasons. It is likely that this result was limited by the small sample size. Only 5 replicates per genotype were analyzed and this increases the variability in the data points which can lead to non-significant results. Another reason could be that the quantification of mature neurons might have been too far away from the region affected by the infarct and hence its effect is hence not detected. Concerning the density of mature neurons in the cortex, no significant difference was found between the two brain hemispheres in this region. This result could also be caused by the same reasons mentioned above. This study was also limited by the brain tissue not always being easy to quantify, as the brain sections could be folded and there were sometimes holes in the tissue. This was especially the case for the brain sections from the cortex, and these holes were removed from the total area when the cell density was calculated. The immunostaining in the KO mice was also often worse and it was easier to analyze the WT sections. NeuN was used as a marker of mature neurons. During the optimalization of the method, the proliferation marker BrdU was also used to stain cells to check for the presence of proliferating neurons which had then matured after HI. No overlap was found, and it would also be unlikely to find this 7 days post HI, as the maturation of neurons has been shown to take around one month in the adult brain rodents[65].

5.2.2 THE EFFECT OF LACTATE ON MITOCHONDRIAL MORPHOLOGY AND NUMBER

Lactate and the activation of HCAR1 has shown to have positive effects on the brain, which includes neurogenesis and enhanced brain function [27]. Recent studies have also demonstrated that exercise and the rise of lactate levels in the blood induces the formation of new mitochondria, which is very important for mitochondrial function in cells [66], [67].

Aim 2 of this study was to test effect of extracellular lactate on mitochondrial size and density in neurons differentiated from neurosphere cultures. Lactate has metabolic effects in cells and activates intracellular pathways in two ways. When lactate is added to the media, it can enter the cell through transmembrane transport through the MCTs. Lactate can furthermore be converted into pyruvate which enters the mitochondria and fuels ATP production. Alternatively, lactate can bind to the HCAR1 receptor on the outside of the cell and activate different signaling cascades[8]. Since lactate and the HCAR1 receptor are linked to energy metabolism and the activity of neurons, it is interesting to study how they also can affect mitochondria morphology and number. However, none of the analyses performed in this study showed a significant difference in the number or the size of the mitochondria in the treated and the control cells. It is possible that other experimental setups would have led to a difference. For example other lactate concentrations or longer durations of lactate treatment.

Based on previous research, it is not unreasonable to expect that metabolites can affect mitochondrial dynamics. In a study by Pekkurnaz et al., they examined how nutrient availability affected mitochondrial mobility in rat hippocampal neurons. They found that higher levels of glucose and the activation of the OGT enzyme slowed down the mobility of the mitochondria and that the mitochondria would accumulate in regions of the axon where the glucose levels were more elevated and allow for an efficient metabolic response [15], [68].
One of the initial sub aim of this thesis was to study mitochondria mobility in HCAR1 KO and WT mice using live imaging, but this was not performed due to problems with the proliferation of the neurospheres.

Limitations of the mitochondrial imaging analysis

The mice used in this study were found to be heterozygous HCAR1 KO/WT mice and the effect of HCAR1 could therefore not be studied.

The method used to visualize the mitochondria in the cell was through immunocytochemistry. This means that the quantification of mitochondria is highly dependent on the specificity of the antibodies used. Unspecific binding of the antibodies can lead to other parts of the cells being stained and give misleading results. In addition, the resolution is not good enough to be able to differentiate the individual mitochondria which are located very close together. This method could have been improved by taking images with higher resolution (e.g by using super-resolution imaging techniques), although it is a more time consuming and demanding method that is beyond the scope of this thesis.

5.2.3. Expression of mitochondrial proteins in brain tissue affected by HI

To further test the effect of HCAR1, protein expression was measured in brain tissue samples from P9 mice 6 hours after induced HI. These results did not show a significant change in the expression of TOMM20, but the COX4 expression showed an increasing trend in the WT mice compared to the KO mice. This increase was present in both contra and ipsi sides of the brain and was hence independent of HI. However, this analysis was limited by a low number of samples (only two samples for WT contra). These data therefore need to be confirmed by repeated experiments containing more samples before any conclusions can be made.

TOMM20 is a translocase on the outer membrane of the mitochondria and is used as a standard marker to stain all mitochondria independently of the function [49]. However, COX4 is a subunit of the cytochrome c oxidase, the terminal electron acceptor in the electron transport chain, and is therefore directly linked to the respiration in cells [52].

A study has looked at the two isoforms of COX4 and found that cells with a downregulation of the COX4-1 isomer compensates with an upregulation of the COX4-2 isomer[52]. Hence although these results could suggest that mice with HCAR1 have higher respiration than KO mice, it could also be that the cells have compensated the downregulation of COX4-1 expression with an upregulation in the expression of the COX4-2 isomer in the KO mice. As COX4-2 is preferentially expressed under hypoxic conditions, and the mice only had 6 hours

of rest before termination, it is probable that the COX4-2 is higher than the COX4-1 expression.

In relation to aim 1, we think that the reduced number of mature cells is caused by neural death in the KO mice after HI. We know that HCAR1 is involved in the activation of neural proliferation after HI[32], but perhaps it is also involved in other signaling pathways such as the regulation of energy metabolism when energy levels are low. HCAR1 could hence be linked to an up- or down- regulation of COX4. Furthermore, some studies have shown that COX4 can be linked to cell apoptosis[69]. As it is an important part of the electron transport chain in the mitochondria, it is responsible of generating a large amount of ATP. However, under stressed conditions, such as hypoxia, the ETC generates reactive oxygen species which can cause cell damage and trigger apoptosis of cells. During cerebral ischemia for example, COX first goes through an ischemic starvation phase in which the tissue is deprived from oxygen which is COX' terminal substrate for respiration. This leads to reduced ATP production, elevated ADP levels and an increase in mitochondrial calcium. In the final stage there is mitochondrial failure and a drastic reduction in the activity of COX. This ends up with energy failure and cell death. Based on this research, a reduced expression of COX4 could be a trigger for neuronal cell death and based on the results of this study HCAR1 could be involved in this signaling pathway. The effect of HCAR1 on the regulation of energy metabolism can be further studied by measuring protein expression of COX4-2. An alternative to brain tissue is to culture neurospheres derived from KO and WT mice and study the presence of COX4-1 and COX4-2 with immunocytochemistry experiments. This model will also make it easier to test the cells with lactate to see a more prominent effect of HCAR1 on respiration. Another method could be to measure respiration directly using a Seahorse analyzer.

In this study, the Seahorse analysis been used to evaluate the metabolism of lactate and glucose in HCAR1 KO cells. This was done to study the effect of the activation of the receptor on retinal glial cells [70]. This method could also be applied here to directly measure the oxygen consumption of WT and HCAR1 KO neurons from differentiated neurospheres.

Limitations of the analysis of mitochondrial protein levels

As described above, an important limitation here is the low number of samples. This study should be repeated with more samples. Further, the vinculin that was used as a control to the TOMM20 antibody showed weak bands on the blot. A weak signal can be due to low antibody concentration, a low exposure time or too much blocking solution or different sample loading. However, TOMM20 from the same blot had a strong signal and had the same amount of loaded sample, and the reason is probably due to the exposure time. The antibodies ACADM and ACADVL did not show any bands in this experiment. They did show a signal during the testing experiments, but they needed further optimalization and due to limited time, they could not be included in this study.

The mice used in this experiment were WT and KO mice which had 6 hours recovery after HI. These were the samples which were available, although it would have been interesting to also analyze samples from other timepoints, for instance closer to the day 7, when mice were fixed for immunohistochemistry (Aim 1).

6. Conclusion and future perspectives

The main aim of this thesis was to study the effect of lactate and the role of the lactate receptor HCAR1 on mitochondrial dynamics and on neuronal survival after HI.

This study has revealed that mice lacking HCAR1 have decreased survival of mature neurons after HI than the mice having the lactate receptor. This study also indicated, albeit with limited statistical power, a reduced protein expression of COX4 in brain tissue in KO mice after HI. Based on these findings, it is possible that HCAR1 could have a role in regulating energy metabolism when energy levels are low by up- or downregulating COX4 expression. In addition to repeating these experiments with more samples, it would be interesting to test other mitochondrial markers, including the markers we attempted to use here (ACADVL and ACADM). We could also test markers for mitochondrial fusion and fission. This could be another way of testing effects on mitochondrial dynamics. Although we did not find an effect of lactate on mitochondrial density and number in this study, it would be interesting to test whether there are differences between HCAR1 KO and WT neurons in fusion and fission proteins.

Overall, this study shows that HCAR1 is found to not only be important for brain tissue regeneration, but also for neuronal survival after HI. Further investigations are needed to see if HCAR1 could have similar effects in humans to find new and effective treatments. Recent studies have found that lactate has shown have a neuroprotective role in rats [30], and our group is currently studying HCAR1 in organotypic human brain slices. It is possible that lactate could be a treatment in for neonatal hypoxia-ischemia and after stroke in elderly people.

7. References

[1] P. Brodal, *The central nervous system: Structure and function (4th ed.)*. 2010.

[2] O. Sand, Ø. Sjaastad V., and E. Haug, *Menneskets fysiologi*, 2nd ed. Oslo: Gyldendal, 2014.

[3] F. Gage, "Adult neurogenesis in mammals," *Current Opinion in Molecular Therapeutics*, vol. 8, no. 4. pp. 345–351, Aug. 2006. doi: 10.1126/science.aav6885.

[4] F. S. Gilbert, *Developmental Biology*, 10th ed., vol. 3. Sinauer Associates, Incorporated Publishers, 2014.

[5] B. Alberts, A. Johnson, J. Lewis, M. Raff, K. Roberts, and P. Walter, *Molecular Biology of the Cell*, 4th ed. Garland Science , 2002.

[6] P. Mergenthaler, U. Lindauer, G. A. Dienel, and A. Meisel, "Sugar for the brain: The role of glucose in physiological and pathological brain function," *Trends in Neurosciences*, vol. 36, no. 10. pp. 587–597, Oct. 2013. doi: 10.1016/j.tins.2013.07.001.

[7] A. F. MacAskill and J. T. Kittler, "Control of mitochondrial transport and localization in neurons," *Trends in Cell Biology*, vol. 20, no. 2. pp. 102–112, Feb. 2010. doi: 10.1016/j.tcb.2009.11.002.

[8] P. J. Magistretti and I. Allaman, "Lactate in the brain: From metabolic end-product to signalling molecule," *Nature Reviews Neuroscience*, vol. 19, no. 4. Nature Publishing Group, pp. 235–249, Apr. 01, 2018. doi: 10.1038/nrn.2018.19.

[9] B. Alberts *et al.*, *Essential Cell Biology Fourth Edition*. 2014.

[10] J. E. Rinholm and L. H. Bergersen, "White matter lactate - Does it matter?," *Neuroscience*, vol. 276. Elsevier Ltd, pp. 109–116, Sep. 12, 2014. doi: 10.1016/j.neuroscience.2013.10.002.

[11] J. E. Rinholm *et al.*, "Movement and structure of mitochondria in oligodendrocytes and their myelin sheaths," *Glia*, vol. 64, no. 5, pp. 810–825, May 2016, doi: 10.1002/glia.22965.

[12] A. F. MacAskill *et al.*, "Miro1 Is a Calcium Sensor for Glutamate Receptor-Dependent Localization of Mitochondria at Synapses," *Neuron*, vol. 61, no. 4, pp. 541–555, Feb. 2009, doi: 10.1016/j.neuron.2009.01.030.

[13] A. F. MacAskill, T. A. Atkin, and J. T. Kittler, "Mitochondrial tracking and the provision of energy and calcium buffering at excitatory synapses," *European Journal of Neuroscience*, vol. 32, no. 2, pp. 231–240, Jul. 2010, doi: 10.1111/j.1460-9568.2010.07345.x.

[14] S. L. Mironov, "ADP regulates movements of mitochondria in neurons," *Biophys J*, vol. 92, no. 8, pp. 2944–2952, 2007, doi: 10.1529/biophysj.106.092981.

[15] G. Pekkurnaz, J. C. Trinidad, Wang Xinnan, Kong Dong, and Schwarz Thomas L., "Glucose regulates mitochondrial motility via Milton modification by O-GlcNAc transferase," *Cell*, pp. 54–68, 2014, doi: https://doi.org/10.1016/j.cell.2014.06.007.

[16] A. B. Knott and E. Bossy-Wetzel, "Impairing the mitochondrial fission and fusion balance: A new mechanism of neurodegeneration," in *Annals of the New York Academy of Sciences*, Blackwell Publishing Inc., 2008, pp. 283–292. doi: 10.1196/annals.1427.030.

[17] Y. J. Liu, R. L. McIntyre, G. E. Janssens, and R. H. Houtkooper, “Mitochondrial fission and fusion: A dynamic role in aging and potential target for age-related disease,” *Mech Ageing Dev*, vol. 186, Mar. 2020, doi: 10.1016/j.mad.2020.111212.
[18] D. Yang *et al.*, “Mitochondrial Dynamics: A Key Role in Neurodegeneration and a Potential Target for Neurodegenerative Disease,” *Frontiers in Neuroscience*, vol. 15. Frontiers Media S.A., Apr. 12, 2021. doi: 10.3389/fnins.2021.654785.
[19] B. S. Ferguson, M. J. Rogatzki, M. L. Goodwin, D. A. Kane, Z. Rightmire, and L. B. Gladden, “Lactate metabolism: historical context, prior misinterpretations, and current understanding,” *European Journal of Applied Physiology*, vol. 118, no. 4. Springer Verlag, pp. 691–728, Apr. 01, 2018. doi: 10.1007/s00421-017-3795-6.
[20] G. Brooks, “Lactate:Glycolytic End Product and Oxidative Substrate During Sustained Exercise in Mammals — The ‘Lactate Shuttle,’” in *Comparative Physiology and Biochemistry - Current Topics and Trends*, 1985, pp. 208–218. doi: 10.1007/978-3-642-70610-3_15.
[21] G. A. Brooks, “The Science and Translation of Lactate Shuttle Theory,” *Cell Metabolism*, vol. 27, no. 4. Cell Press, pp. 757–785, Apr. 03, 2018. doi: 10.1016/j.cmet.2018.03.008.
[22] H. de C. Abrantes *et al.*, “The lactate receptor HCAR1 modulates neuronal network activity through the activation of Gα and Gβγ subunits,” *Journal of Neuroscience*, vol. 39, no. 23, pp. 4422–4433, Jun. 2019, doi: 10.1523/JNEUROSCI.2092-18.2019.
[23] D. M. Rosenbaum, S. G. F. Rasmussen, and B. K. Kobilka, “The structure and function of G-protein-coupled receptors,” *Nature*, vol. 459, no. 7245. pp. 356–363, May 21, 2009. doi: 10.1038/nature08144.
[24] T. P. Brown and V. Ganapathy, “Lactate/GPR81 signaling and proton motive force in cancer: Role in angiogenesis, immune escape, nutrition, and Warburg phenomenon,” *Pharmacology and Therapeutics*, vol. 206. Elsevier Inc., Feb. 01, 2020. doi: 10.1016/j.pharmthera.2019.107451.
[25] K. Ahmed *et al.*, “An Autocrine Lactate Loop Mediates Insulin-Dependent Inhibition of Lipolysis through GPR81,” *Cell Metab*, vol. 11, no. 4, pp. 311–319, Apr. 2010, doi: 10.1016/j.cmet.2010.02.012.
[26] K. H. Lauritzen *et al.*, “Lactate receptor sites link neurotransmission, neurovascular coupling, and brain energy metabolism,” *Cerebral Cortex*, vol. 24, no. 10, pp. 2784–2795, Oct. 2014, doi: 10.1093/cercor/bht136.
[27] C. Morland *et al.*, “Exercise induces cerebral VEGF and angiogenesis via the lactate receptor HCAR1,” *Nat Commun*, vol. 8, May 2017, doi: 10.1038/ncomms15557.
[28] M. Briquet *et al.*, “Activation of lactate receptor HCAR1 down-modulates neuronal activity in rodent and human brain tissue,” *Journal of Cerebral Blood Flow and Metabolism*, vol. 42, no. 9, pp. 1650–1665, Sep. 2022, doi: 10.1177/0271678X221080324.
[29] L. J. Millar, L. Shi, A. Hoerder-Suabedissen, and Z. Molnár, “Neonatal hypoxia ischaemia: Mechanisms, models, and therapeutic challenges,” *Frontiers in Cellular Neuroscience*, vol. 11. Frontiers Media S.A., May 08, 2017. doi: 10.3389/fncel.2017.00078.
[30] H. Roumes *et al.*, “Neuroprotective role of lactate in rat neonatal hypoxia-ischemia,” *Journal of Cerebral Blood Flow and Metabolism*, vol. 41, no. 2, pp. 342–358, Feb. 2021, doi: 10.1177/0271678X20908355.
[31] I. D. Á. Tassinari *et al.*, “Lactate Administration Reduces Brain Injury and Ameliorates Behavioral Outcomes Following Neonatal Hypoxia–Ischemia,” *Neuroscience*, vol. 448, pp. 191–205, Nov. 2020, doi: 10.1016/j.neuroscience.2020.09.006.

[32] L. Kennedy *et al.*, “Lactate receptor HCAR1 regulates neurogenesis and microglia activation after neonatal hypoxia-ischemia,” *Elife*, vol. 11, Aug. 2022, doi: 10.7554/eLife.76451.
[33] R. Soares *et al.*, “The neurosphere assay: An effective in vitro technique to study neural stem cells,” *Neural Regeneration Research*, vol. 16, no. 11. Wolters Kluwer Medknow Publications, pp. 2229–2231, Nov. 01, 2021. doi: 10.4103/1673-5374.310678.
[34] M. Picard, S. O. Shirihai, J. B. Gentil, and Y. Burelle, “Mitochondrial morphology transitions and functions: implications for retrograde signaling?,” *Am J Physiol Regul Integr Comp Physiol*, 2013, doi: https://doi.org/10.1152/ajpregu.00584.2012.
[35] K. Ahmed *et al.*, “An Autocrine Lactate Loop Mediates Insulin-Dependent Inhibition of Lipolysis through GPR81,” *Cell Metab*, vol. 11, no. 4, pp. 311–319, Apr. 2010, doi: 10.1016/j.cmet.2010.02.012.
[36] SinoBiological, “What is Immunocytochemistry (ICC)?” https://www.sinobiological.com/category/what-is-icc (accessed Apr. 23, 2023).
[37] A. H. Coons, H. J. Creech, R. N. Jones, and E. Berliner, “The Demonstration of Pneumococcal Antigen in Tissues by the Use of Fluorescent Antibody1,” *The Journal of Immunology*, vol. 45, no. 3, pp. 159–170, Nov. 1942, doi: 10.4049/jimmunol.45.3.159.
[38] S. Magaki, S. A. Hojat, B. Wei, A. So, and W. H. Yong, “An introduction to the performance of immunohistochemistry,” in *Methods in Molecular Biology*, Humana Press Inc., 2019, pp. 289–298. doi: 10.1007/978-1-4939-8935-5_25.
[39] R. Soares *et al.*, “Isolation and expansion of neurospheres from postnatal (P1−3) mouse neurogenic niches,” *Journal of Visualized Experiments*, vol. 2020, no. 159, May 2020, doi: 10.3791/60822.
[40] S. Gil-Perotín, M. Duran-Moreno, A. Cebrián-Silla, M. Ramírez, P. García-Belda, and J. M. García-Verdugo, “Adult neural stem cells from the subventricular zone: A review of the neurosphere assay,” *Anatomical Record*, vol. 296, no. 9, pp. 1435–1452, Sep. 2013, doi: 10.1002/ar.22746.
[41] R. Thavarajah, V. K. Mudimbaimannar, J. Elizabeth, U. K. Rao, and K. Ranganathan, “Chemical and physical basics of routine formaldehyde fixation,” *Journal of Oral and Maxillofacial Pathology*, vol. 16, no. 3. pp. 400–405, Sep. 2012. doi: 10.4103/0973-029X.102496.
[42] A. J. Hobro and N. I. Smith, “An evaluation of fixation methods: Spatial and compositional cellular changes observed by Raman imaging,” *Vib Spectrosc*, vol. 91, pp. 31–45, Jul. 2017, doi: 10.1016/j.vibspec.2016.10.012.
[43] R. A. DeGiosio, M. J. Grubisha, M. L. MacDonald, B. C. McKinney, C. J. Camacho, and R. A. Sweet, “More than a marker: potential pathogenic functions of MAP2,” *Front Mol Neurosci*, vol. 15, Sep. 2022, doi: 10.3389/fnmol.2022.974890.
[44] J. , R. Mullen, R. , C. Buck, and M. , A. Smith, “NeuN, a neuronal specific nuclear protein in vertebrates”, doi: https://doi.org/10.1242/dev.116.1.201.
[45] G. F. Gebhart and R. F. Schmidt, “Neurofilament Protein NF200,” in *Encyclopedia of Pain*, R. F. Gebhart Gerald F. and Schmidt, Ed., Berlin, Heidelberg: Springer Berlin Heidelberg, 2013, p. 2046. doi: 10.1007/978-3-642-28753-4_201396.
[46] W. Schubert, V. Coskun, M. Tahmina, M. S. Rao, M. B. Luskin, and Z. Kaprielian, “Characterization and Distribution of a New Cell Surface Marker of Neuronal Precursors,” 2000.
[47] S. S. Easter, L. S. Ross, and A. Frankfurtep, “Initial Tract Formation in the Mouse Brain,” 1993.

[48] S. P. Memberg and A. K. Hall, “Dividing neuron precursors express neuron-specific tubulin,” *J Neurobiol*, vol. 27, no. 1, pp. 26–43, 1995, doi: https://doi.org/10.1002/neu.480270104.
[49] S. H. Park, A. R. Lee, K. Choi, S. Joung, J. B. Yoon, and S. Kim, “TOMM20 as a potential therapeutic target of colorectal cancer,” *BMB Rep*, vol. 52, no. 12, pp. 712–717, 2019, doi: 10.5483/BMBRep.2019.52.12.249.
[50] A. P. Y. Ma *et al.*, “Suppression of ACADM-mediated fatty acid oxidation promotes hepatocellular carcinoma via aberrant CAV1/SREBP1 signaling,” *Cancer Res*, vol. 81, no. 13, pp. 3679–3692, Jul. 2021, doi: 10.1158/0008-5472.CAN-20-3944.
[51] T. Chen *et al.*, “Novel ACADVL variants resulting in mitochondrial defects in long-chain acyl-CoA dehydrogenase deficiency,” *J Zhejiang Univ Sci B*, vol. 21, no. 11, pp. 885–896, Nov. 2020, doi: 10.1631/jzus.B2000339.
[52] L. Douiev, C. Miller, S. Ruppo, H. Benyamini, B. Abu-Libdeh, and A. Saada, “Upregulation of cox4-2 via hif-1α in mitochondrial cox4-1 deficiency,” *Cells*, vol. 10, no. 2, pp. 1–16, Feb. 2021, doi: 10.3390/cells10020452.
[53] T. Mahmood and P. C. Yang, “Western blot: Technique, theory, and trouble shooting,” *N Am J Med Sci*, vol. 4, no. 9, pp. 429–434, Sep. 2012, doi: 10.4103/1947-2714.100998.
[54] M. Minsky, “Memoir on inventing the confocal scanning microscope,” *Scanning*, vol. 10, no. 4, pp. 128–138, 1988, doi: https://doi.org/10.1002/sca.4950100403.
[55] K. Thorn, “A quick guide to light microscopy in cell biology,” *Mol Biol Cell*, vol. 27, no. 2, pp. 219–222, Jan. 2016, doi: 10.1091/mbc.E15-02-0088.
[56] T. J. Collins, “ImageJ for microscopy,” *Biotechniques*, vol. 43, no. 1S, pp. S25–S30, Jul. 2007, doi: 10.2144/000112517.
[57] I. Buchwalow, V. Samoilova, W. Boecker, and M. Tiemann, “Multiple immunolabeling with antibodies from the same host species in combination with tyramide signal amplification,” *Acta Histochem*, vol. 120, no. 5, pp. 405–411, Jul. 2018, doi: 10.1016/j.acthis.2018.05.002.
[58] G. Scherrer *et al.*, “VGLUT2 expression in primary afferent neurons is essential for normal acute pain and injury-induced heat hypersensitivity,” *Proc Natl Acad Sci U S A*, vol. 107, no. 51, pp. 22296–22301, Dec. 2010, doi: 10.1073/pnas.1013413108.
[59] A. Durukan and T. Tatlisumak, “Acute ischemic stroke: Overview of major experimental rodent models, pathophysiology, and therapy of focal cerebral ischemia,” *Pharmacol Biochem Behav*, vol. 87, no. 1, pp. 179–197, May 2007, doi: 10.1016/j.pbb.2007.04.015.
[60] P. R. Krafft *et al.*, “Etiology of stroke and choice of models,” *International Journal of Stroke*, vol. 7, no. 5. pp. 398–406, Jul. 2012. doi: 10.1111/j.1747-4949.2012.00838.x.
[61] S. Leverz, “ANOXIC-ISCE C ENCEPHALOPATHY IN RATS.”
[62] J. J. Kurinczuk, M. White-Koning, and N. Badawi, “Epidemiology of neonatal encephalopathy and hypoxic-ischaemic encephalopathy,” *Early Human Development*, vol. 86, no. 6. pp. 329–338, Jun. 2010. doi: 10.1016/j.earlhumdev.2010.05.010.
[63] V. Donega, C. T. J. Van Velthoven, C. H. Nijboer, A. Kavelaars, and C. J. Heijnen, “The endogenous regenerative capacity of the damaged newborn brain: Boosting neurogenesis with mesenchymal stem cell treatment,” *Journal of Cerebral Blood Flow and Metabolism*, vol. 33, no. 5. pp. 625–634, May 2013. doi: 10.1038/jcbfm.2013.3.
[64] X. Castillo *et al.*, “A probable dual mode of action for both L-and D-lactate neuroprotection in cerebral ischemia,” *Journal of Cerebral Blood Flow and Metabolism*, vol. 35, no. 10, pp. 1561–1569, Oct. 2015, doi: 10.1038/jcbfm.2015.115.
[65] I. Dori, C. Bekiari, I. Grivas, A. Tsingotjidou, and G. C. Papadopoulos, “Birth and death of neurons in the developing and mature mammalian brain,” *The International*

journal of developmental biology, vol. 66, no. 123. NLM (Medline), pp. 9–22, 2022. doi: 10.1387/ijdb.210139id.

[66] J. Park, J. Kim, and T. Mikami, "Exercise-Induced Lactate Release Mediates Mitochondrial Biogenesis in the Hippocampus of Mice via Monocarboxylate Transporters," *Front Physiol*, vol. 12, Sep. 2021, doi: 10.3389/fphys.2021.736905.

[67] J. L. Steiner, E. Angela Murphy, J. L. McClellan, M. D. Carmichael, and J. Mark Davis, "Exercise training increases mitochondrial biogenesis in the brain," *J Appl Physiol*, vol. 111, pp. 1066–1071, 2011, doi: 10.1152/japplphysiol.00343.2011.-Increased.

[68] A. Agrawal, G. Pekkurnaz, and E. F. Koslover, "Spatial control of neuronal metabolism through glucose-mediated mitochondrial transport regulation," 2018, doi: 10.7554/eLife.40986.001.

[69] M. Hüttemann *et al.*, "Regulation of mitochondrial respiration and apoptosis through cell signaling: Cytochrome c oxidase and cytochrome c in ischemia/reperfusion injury and inflammation," *Biochimica et Biophysica Acta - Bioenergetics*, vol. 1817, no. 4. pp. 598–609, Apr. 2012. doi: 10.1016/j.bbabio.2011.07.001.

[70] R. Vohra, B. I. Aldana, H. Waagepetersen, L. H. Bergersen, and M. Kolko, "Dual properties of lactate in müller cells: The effect of GPR81 activation," *Invest Ophthalmol Vis Sci*, vol. 60, no. 4, pp. 999–1008, Mar. 2019, doi: 10.1167/iovs.18-25458.

8. Appendix

Section A: Reagents and consumables

Table A1: Reagents, producer and catalogue number

Reagent	**Producer**	**Catalogue number**
Normal goal serum (NGS)	Sigma-Aldrich	69023
Bovine serum albumin (BSA)	Saween & Werner	B2000-500
DPBS(1X)	Gibco	14190-094
Phosphate buffered saline tablets	Sigma Aldrich	P4417
ProLong Glass Antifade Mountant	Thermo Fisher Scientific	P36930
TritonTM X-100	Sigma-Aldrich	T8787
10x Tris/Glycine/SDS buffer	Bio-Rad Laboratories	16110732
Skim Milk Powder	Sigma-Aldrich	70166
Trypsin-EDTA, phenol red	Thermo Fisher	25200056
Penicillin-Streptomycin-Glutamine	Thermo Fisher	10378016
Triton-TM X-100	Sigma Aldrich	X100
Halt™ Protease and Phosphatase Inhibitor Single-Use Cocktail (100X)	Thermo Fisher Scientific	78442
TWEEN 20	Sigma-Aldrich	P1379
4% Paraformaldehyde solution	Thermo Fisher Scientific	sc-281692
Restore PLUS Western Blot Stripping Buffer	Thermo Scientific	46430

Table A2: Consumables, producer and catalogue number

Consumables	Producer	Catalogue number
SuperSignal West Femto Maximum Sensitivity Substrate	Thermo Scientific	34095
4-20% Criterion TGX Precast Gels, 18 well comb, 30 uL, 1.0 mm	Bio Rad	5671094
Trans-Blot Turbo Transfer Pack, Mido format 0.2 um PVDF	Bio Rad	1704157
Ladder Precision Plus protein dual color standards	Bio Rad	1610374
Super normal size PAP pen	Electron Microscopy Sciences	71310
Superfrost Plus microscope slides	VWR	631-9483
Carl Zeiss Immersol Immersion Oil	Thermo Fisher	10539438

Section B: Antibodies

Table B1: Antibodies for immunohistochemistry

Antibody	Host	Dilution	Producer	Catalogue nr.
MAP2	Rabbit	1:400	Merck Millipore	AB5622
NeuN	Mouse	1:400	Merck Millipore	MAB377
NF200	Chicken	1:5000	Invitrogen	11548801
BrdU	Rat	1:200	Abcam	ab6326
Alexa fluor 488 anti-rabbit lgG (H+L)	Goat	1:1000		A11008
Goat anti-Mouse lgG (H+L) Alexa Fluor 555	Goat	1:1000	Thermo Fisher	A21422
Goat anti-rat lgG(H+L), Alexa Fluor 633 anti-rat	Goat	1:1000	Thermo Fisher	A21070

DAPI (1:5000), Sigma, #D-9542-1MG

Table B2: Antibodies for immunocytochemistry

Antibody	**Host**	**Dilution**	**Producer**	**Catalogue nr.**
MAP2	Rabbit	1:400	Merck Millipore	AB5622
NeuN	Mouse	1:400	Merck Millipore	MAB377
NF200	Chicken	1:5000	Invitrogen	11548801
TOMM20	Rabbit	Abcam	Abcam	Ab78547
ACADM	Mouse	1:1000	Abcam	ab110296
ACADVL	Mouse	1:200	Merck Millipore	ab110285
COX4	Mouse	1:300	Invitrogen	GT6310
TUJ1	Mouse	1:400	R&D systems	MAB1195
Alexa fluor 488 anti-rabbit lgG (H+L)	Goat	1:1000		A11008
Goat anti-Mouse lgG (H+L) Alexa Fluor 555	Goat	1:1000	ThermoFischer	A21422
Alexa Fluor 633 anti-chicken	Goat	1:1000	-	-

Table B3: Antibodies for western blotting

Antibody	**Host**	**Dilution**	**Producer**	**Catalogue nr.**
TOMM20	Rabbit	1:1000	Abcam	Ab78547
ACADM	Mouse	1:8000	Abcam	ab110296
ACADVL	Mouse	1:1000	Merck Millipore	ab110285
COX4	Mouse	1:1000	Invitrogen	GT6310
Monoclonal Anti-vincullin	Mouse	1:10000	Merck	V9131
Donkey Anti-Mouse lgG H&L	Donkey	1:20000	Abcam	Ab6820
Donkey Anti-Rabbit lgG H&L	Donkey	1:20000	Abcam	Ab6802

Section C: Media components, solutions and buffers

Media for neurosphere proliferation and differentiation

Coating:
Poly-D-Lysine, 10 ug/mL(ThermoFischer, A3890401)

Proliferation medium:
• DMEM/F12 (ThermoFisher, #21331-020)
• Glutamax supplement (ThermoFisher, #35050061)
• N2 supplement (100X) (Fisher Scientific, #17502001)
• B27 without Vit A (ThermoFisher, #12587010)
• Recombinant Human EGF Protein, CF (R&D systems, #236-EG)
• Recombinnat human FGFbasic (Peprotech, #45002B)

Differentiation medium:
Proliferation medium without EGF and bFGF

Dissociation medium:
5% trypsin-EDTA

Tryspin activation for neurosphere culture:
1% BSA in PBS

Solutions and buffers

PBS (0,01M, pH 7,4)
Citrate buffer (10 mM, pH 6,0)

Block solution IHC:
• 10% Normal goat serum (NGS)
• 1% Bovine serum albumin (BSA)
• 0,5 % Triton X-100
• Diluted in PBS

Primary and secondary antibody solution:
• 3 % NGS
• 1 % BSA
• 0,5 % Triton X-100
• Diluted in PBS

Block solution for Western blotting:
- 5% skim milk powder
- Diluted in PBS-T

PBS-T:
- 0,1% Tween-20
- Diluted in PBS

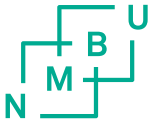

Norges miljø- og biovitenskapelige universitet
Noregs miljø- og biovitskapelege universitet
Norwegian University of Life Sciences

Postboks 5003
NO-1432 Ås
Norway